



Technical University of Munich  
Chair of Transportation Systems Engineering

Master's Thesis

# **Influence of Connected and Cooperative Vehicles on Virtual Right of Way Performance in Mixed Traffic**

**Author:**

Michael Winsor

**Matriculation No:**

03694760

**Supervised by:**

Dr. Tao Ma (TUM)  
M.Sc. Meng Xie (TUM CREATE)

**Chair Head:**

Prof. Dr. Constantinos Antoniou

June 4, 2020

## **Acknowledgments**

This work was financially supported by the National Research Foundation (NRF) Singapore under its Campus for Research Excellence And Technological Enterprise (CREATE) program. It is thanks to their endorsement that this thesis was possible. On the simulation front, PTV Group's support in providing the academic license for Vissim was instrumental in enabling this research. I would also like to thank my mentor and colleague, Meng Xie, whose work and expertise in Virtual Right of Way helped to resolve many of the issues I experienced along the way. My thanks also go to my supervisor, Dr. Tao Ma, for his dedication and support. His insights into the concepts and results of this research provided a fresh perspective that was tremendously helpful. Most importantly, I would like to thank my fiancée, Vân. Her patience and unwavering support over the past months have contributed far more to this work than is possible to measure.

## Abstract

Providing public transportation with priority over general traffic is an important measure to provide reliable services. However, balancing the priority of public transit and general traffic must be done carefully. Exclusive bus lanes, for example, (EBLs) improve bus performance but are not suitable in all situations. A dynamic bus lane known as Virtual Right of Way (VROW) has been proposed to better balance the road space between buses and private vehicles. Using vehicle-to-everything (V2X) communication, VROW only requests vehicles in the bus lane to change lanes if they will delay the bus operations. In dense traffic, however, there are few available gaps to safely accommodate VROW lane change requests. Furthermore, it is not known how different compliance rates of human drivers will affect VROW performance. A cooperative driving algorithm has thus been developed to facilitate vehicle lane changes due to VROW requests in both dense and free-flowing mixed traffic. The proposed driving algorithm creates gaps by cooperative lane changes and cooperative acceleration control. The algorithm was integrated with VROW and simulated in a Vissim model of an arterial corridor in Singapore. Results showed that cooperative driving is able to supplement VROW operation under dense traffic conditions, but free-flow conditions showed no significant improvements. Acceleration and jerk were well controlled by the algorithm, although some issues remain when handing control back to Vissim's driving behavior model. Different penetration rates of cooperative vehicles in the network also impacted the efficiency of VROW and cooperative driving. At cooperative vehicle penetration rates of 50% and below, no improvements in bus travel times were observed. Bus travel times only improved for the 75% and 100% compliance scenarios. Applying such a cooperative strategy as proposed here to support VROW could, therefore, help to further improve bus reliability and reduce the number of buses required to operate a route, but only provided that there is a high compliance rate from the general traffic.

**Keywords:** Cooperative Driving, Connected Vehicles, Penetration Rate, Public Transport Prioritization, V2V, V2X

## Table of Contents

<b>Abstract</b> .....	<b>i</b>
<b>1. Chapter 1: Introduction</b> .....	<b>1</b>
<b>1.1. Problem Statement</b> .....	<b>1</b>
<b>1.2. Transportation in Singapore</b> .....	<b>2</b>
<b>1.3. The DART System</b> .....	<b>2</b>
<b>1.4. Research Objectives</b> .....	<b>3</b>
<b>1.5. Thesis Structure</b> .....	<b>3</b>
<b>2. Chapter 2: Theoretical Framework</b> .....	<b>5</b>
<b>2.1. Vehicular Communication Technologies</b> .....	<b>5</b>
2.1.1. Vehicle-to-Vehicle Communication .....	5
2.1.2. Vehicle-to-Infrastructure Communication .....	6
2.1.3. Vehicle to Everything Communication .....	7
<b>2.2. Cooperative Driving</b> .....	<b>7</b>
2.2.1. Highway Cooperation .....	8
2.2.2. Urban Roadway Cooperation .....	11
2.2.3. Acceleration and Jerk as Safety and Comfort Parameters .....	12
<b>2.3. Driving Behavior Models</b> .....	<b>13</b>
2.3.1. Car-Following Models .....	13
2.3.2. Lane-Changing Models .....	14
2.3.3. Vissim’s Driving Behavior Model .....	15
<b>2.4. Virtual Right of Way</b> .....	<b>19</b>
<b>3. Chapter 3: Methodology</b> .....	<b>21</b>
<b>3.1. Cooperative Driving Integration with VROW</b> .....	<b>23</b>
<b>3.2. Cooperative Driving Algorithm</b> .....	<b>26</b>
3.2.1. Lane-Changing and Gap Acceptance .....	26
3.2.2. Cooperative Acceleration .....	28
3.2.3. Issues with Vehicle Platooning and Autonomous Vehicles .....	32
<b>4. Chapter 4: Case Study</b> .....	<b>33</b>
<b>4.1. Study Area Simulation Model</b> .....	<b>33</b>
4.1.1. Private Vehicle Modeling.....	33
4.1.2. Public Transport Modelling .....	36
4.1.3. Signal Controllers.....	36
<b>4.2. Model Calibration</b> .....	<b>36</b>
4.2.1. Calibration Metric.....	38
4.2.2. Performance Measures .....	38

4.2.3. Calibration Approach .....	38
4.2.4. Calibration Results .....	39
<b>4.3. Implementation of VROW and Cooperative Driving in Vissim .....</b>	<b>39</b>
<b>4.4. Scenario Definition and Preparation .....</b>	<b>40</b>
<b>5. Chapter 5: Results and Analysis .....</b>	<b>41</b>
<b>5.1. Gap Acceptance.....</b>	<b>41</b>
<b>5.2. Acceleration and Jerk .....</b>	<b>42</b>
5.2.1. Individual Vehicle Control.....	42
5.2.2. Jerk and Acceleration Distributions.....	44
<b>5.3. Vehicle Travel Times.....</b>	<b>46</b>
5.3.1. Northbound Travel Times.....	47
5.3.2. Southbound Travel Times.....	49
<b>5.4. Number of Lane Changes .....</b>	<b>52</b>
<b>5.5. Following Distance Distribution .....</b>	<b>54</b>
<b>5.6. VROW and the Cooperative Driving Algorithm .....</b>	<b>55</b>
<b>6. Chapter 6: Conclusions .....</b>	<b>59</b>
<b>List of References .....</b>	<b>60</b>
<b>List of Abbreviations.....</b>	<b>66</b>
<b>List of Symbols .....</b>	<b>67</b>
<b>List of Figures .....</b>	<b>69</b>
<b>List of Tables .....</b>	<b>71</b>
<b>Declaration Concerning the Master’s Thesis .....</b>	<b>72</b>

# 1. Chapter 1: Introduction

## 1.1. Problem Statement

Cities around the world are faced with growing levels of traffic congestion. While this can be seen as a sign of growth and prosperity to the cities' economies, congestion can also limit further economic growth, impact people's wellbeing, and harm the health of the environment (Zhang and Batterman, 2013). Finding ways to reduce congestion levels is thus critical for the long-term health of cities and the environment, but options to achieve this goal are limited. Due to the limited land availability in cities, building new roads is not a viable option. This is particularly true for the island city-state of Singapore, where the small land area and dense population make finding new space for infrastructure difficult.

Congestion within cities is the result of high traffic volumes using the road network and exceeding its total capacity. It is often caused by a high number of private vehicles commuting to and from work during peak hours. Public bus services have offered more beneficial ways to utilize the road space and reduce the number of private vehicles on the road more efficiently. However, high levels of congestion can undermine these benefits, as buses impeded by traffic are unable to operate reliably and efficiently. Bus prioritization methods have been implemented in many major cities to mitigate this issue. In the case of Singapore, exclusive bus lanes (EBLs) have been deployed across the city as the primary prioritization method for buses. EBLs can drastically improve the reliability of bus services, as they provide a dedicated lane for buses to travel without disturbances from the general traffic. However, low bus frequencies or excessive general traffic demand make them infeasible in many situations.

Some modifications to the EBL concept were instituted to reduce the negative impacts of EBLs on the general traffic while also maintaining a similar level of performance for buses. The Intermittent Bus Lanes (IBL) created a dynamic bus lane that was only activated when a bus was using it (Eichler and Daganzo, 2006; Viegas and Lu, 2000). Yet, it only prevented vehicles from merging into it and did not request vehicles to leave the bus lane once activated. Bus Lanes with Intermittent Priority (BLIP) was also introduced as a dynamic bus lane similar to the IBL. BLIP operated with a fixed clearing distance from the bus and requested all vehicles not using the lane for a turning movement to merge into the adjacent lane. Both systems improved upon the EBL and provided more optimal usage of the road. However, a more optimal clearing distance for the bus can provide similar travel time benefits for buses with less overall disturbances to the general traffic. The Virtual Right of Way (VROW) bus prioritization protocol has thus been proposed to solve this problem.

VROW utilizes vehicle-to-everything (V2X) communication to request lane changes from vehicles expected to delay a bus's operation. It does this through aggregating traffic signal information and relative velocities between preceding vehicles and the bus. Vehicles using the turning lane or vehicles that are traveling on a trajectory that will not interfere with the bus are allowed to stay in the lane, thus reducing the overall impact of the bus on the general traffic. Despite the added benefits, it is not known how the effects of forcing lane changes from vehicles will impact the performance of VROW. Some vehicles may be unwilling to comply with the signal, while others may not find suitable gaps in their adjacent lane to provide the bus with the right of way. As vehicle communication technologies continue to develop, new opportunities for vehicle control and traffic management become possible. Singapore, as a city with advanced traffic management practices, holds the potential to take advantage of these new technologies.

### **1.2. Transportation in Singapore**

Singapore, as an island nation, is particularly constrained in terms of space for infrastructural expansion. Official government data shows that Singapore's expressway network has remained unchanged since 2013, and the arterial road network has only been expanded by 46 km during the same period (Land Transport Authority, 2020b). As an alternative to roadway expansion, the government has taken measures to limit car ownership and implemented congestion pricing on major expressways across the country (Ministry of Transport, 2011). As a result, private vehicle ownership has become expensive for many in Singapore. However, there have also been substantial investments in public transportation infrastructure and priority to service the high captive public transport ridership population (Ministry of Transport, 2013).

Despite these measures, traffic congestion is still a problem. The average speeds on expressways and arterial roads during peak hours are consistently around 60 km/h and 30 km/h, respectively, while the allowed speed limits on expressways are between 80 – 90 km/h and that for arterial roads is between 50 – 60 km/h (Land Transport Authority, 2020a, 2020b). As many people in Singapore rely on buses to move around, finding measures to help improve bus performance can have a significant impact. Factoring in Singapore's extensive use of EBLs, incorporating technologies such as VROW to balance the road space between private and public transport more efficiently can thus help to reduce the high congestion levels in the city.

### **1.3. The DART System**

TUM CREATE is researching the development of a Dynamic and Autonomous Road Transit (DART) system that is intended to create a connected and shared transport system that can complement public bus systems (Rau et al., 2019). It consists of a fleet of modular, electric autonomous vehicles of various sizes that offer more flexible operational capabilities than traditional buses. Depending on current demand, the system can quickly adjust the capacity of

different fixed-route services or even offer on-demand services in situations with very low passenger demand. The DART system incorporates VROW and other technologies such as platooning and signal priorities to attain higher operational speeds while reducing the overall disturbances on general traffic (TUM CREATE, 2020). Figure 1.1 shows the conceptual idea of the DART modules.



Figure 1.1. Concept of the DART system (TUM CREATE, 2020).

#### **1.4. Research Objectives**

There were two main objectives of this research. The first was to develop a cooperative driving algorithm that could support and further improve VROW performance through cooperative lane changes and acceleration adjustments in an urban environment. Essentially, the goal of the algorithm was to create larger gaps in order to assist connected vehicles in moving away from the VROW bus lane, thus helping to reduce delays on the bus caused by vehicles unable to change lanes. Although human drivers who receive the signal may cooperate with VROW, others may not. This leads to the second objective of this report. As human drivers do not always act in the best interest of the overall system, the effects of different compliance rates of human drivers on the performance of VROW buses were also investigated. This is simulated with different proportions of connected and non-connected vehicles in the network. As a secondary objective, the potential for vehicles to form a platoon behind the VROW bus as a way to mitigate delays caused by VROW lane changes was also explored. This would help to further reduce any negative impacts on the general traffic from VROW lane change requests.

#### **1.5. Thesis Structure**

The remainder of this report is divided into five chapters. In the second chapter, a detailed literature review is presented on vehicular communication technologies, cooperative driving, driving behavior models, and VROW. The third chapter contains the methodology for the development of the proposed cooperative driving algorithm as well as how it complements the

operation of VROW. Chapter 4 describes the case study area for simulation in Vissim, the calibration of the developed model, and the preparation of the different scenarios for analyzing the algorithm's performance. The results of the simulation runs are discussed in chapter 5, which explains how the cooperative driving algorithm performed in different compliance scenarios. Lastly, chapter 6 presents the conclusions of the research and highlights potential areas of future work, as well as some limitations of the proposed algorithm.

## **2. Chapter 2: Theoretical Framework**

### **2.1. Vehicular Communication Technologies**

Vehicular communication systems are an extensive topic representing the culmination of the telecommunications and intelligent transportation fields. The research presented in this thesis does not focus on this topic, but it is an underlying technology used for VROW and cooperative driving. As such, an overview of the important topics of vehicular communication technologies is presented here, but it is by no means an exhaustive summary of the field.

Depending on the communication architecture used, vehicular communication systems can be defined as either vehicle-to-vehicle (V2V) or vehicle-to-infrastructure (V2I). A third classification, known as vehicle-to-everything (V2X), represents a system that combines both of these communication types. But whatever the type of system used, vehicles and infrastructure act as nodes that wirelessly send and receive information (Papadimitratos et al., 2008). In order for vehicular communication to work, vehicles must be equipped with some type of on-board unit that receives information. Each onboard unit communicates over a dedicated frequency determined by the ITS-G5 standard to send information regarding the vehicle's position, speed, acceleration, etc. (Strom, 2011).

#### **2.1.1. Vehicle-to-Vehicle Communication**

Vehicular ad hoc networks (VANETs) are a common architecture for V2V communication. They use a decentralized and dynamic architecture to transfer data between vehicles that have joined the network (Reina et al., 2016). VANETs rely on lightweight and reliable data transfer. However, one concern with these systems, particularly in dense traffic settings, is that signals emitted from vehicles will collide and interfere with signals from other vehicles, severely limiting the efficacy of VANETs (Panichpapiboon and Pattara-atikom, 2012). There have been several algorithms proposed to mitigate signal interference from a crowded communication network, but these algorithms are beyond the scope of this research (Feukeu and Zuva, 2020; Panichpapiboon and Pattara-atikom, 2012).

With VANETs, vehicles are able to communicate mainly with their nearest neighboring vehicles. However, one vehicle's information can be passed on through the network by its neighboring vehicles in a process known as multi-hopping (da Costa et al., 2019). This allows vehicles to receive information from vehicles farther downstream and overcome communication range limitations, which is especially limited in urban settings due to signal blockage by buildings. A schematic of the multi-hop concept is shown in Figure 2.1. Cooperative driving algorithms can utilize the multi-hop data to estimate downstream traffic conditions, smooth traffic shockwaves, and form stable vehicle platoons (Jia and Ngoduy, 2016b; Ploeg et al., 2018).

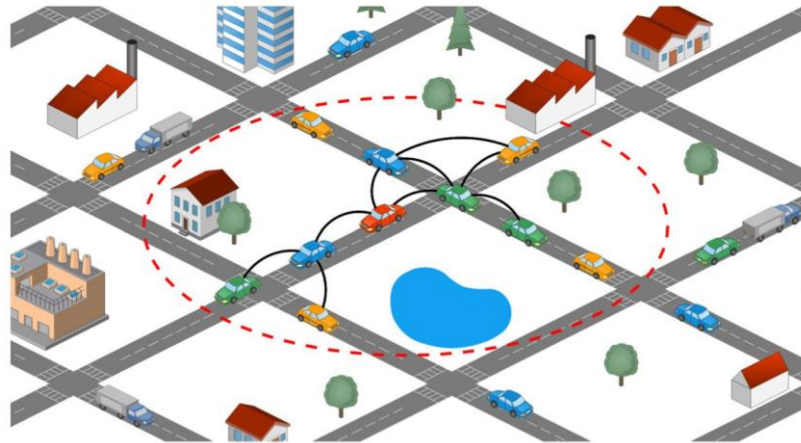


Figure 2.1. Multi-hop data transmission for VANET in urban setting (da Costa et al., 2019).

### 2.1.2. Vehicle-to-Infrastructure Communication

V2I communication depends upon physical infrastructure to transfer data to and from vehicles that are within range. In this case, vehicles do not directly communicate with one another. Implementation of V2I communication can vary depending on the situation, as different types of infrastructure can fulfill different needs. Roadside units (RSUs) are a common communication infrastructure placed along roads to send and receive data with passing vehicles (Ploeg et al., 2018). As seen in figure 2.2, the RSUs connect wirelessly to vehicles and pass the collected vehicle data back to a centralized server for use in traffic control management (Bi et al., 2014). The data collected by RSUs can be used for different purposes. Informing vehicles of downstream traffic conditions or accidents is one such application that can help to improve traffic safety (Bi et al., 2014). RSUs can also be applied to form vehicle platoons in both highway and urban road settings (Ploeg et al., 2018).

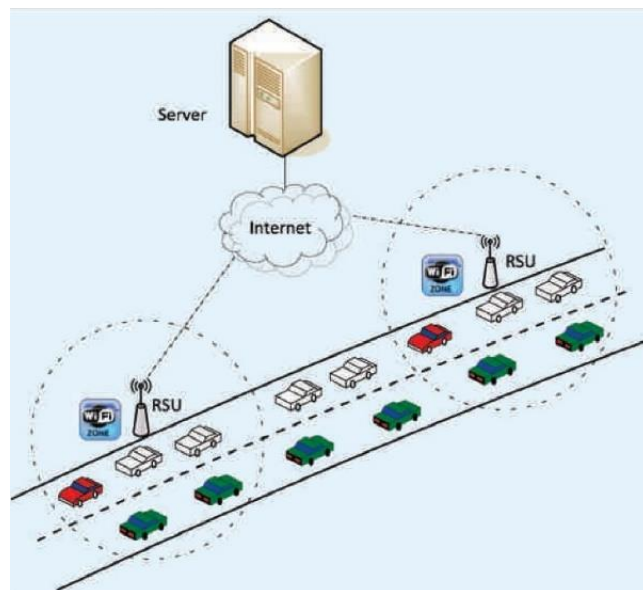


Figure 2.2. V2I communication architecture schematic (Bi et al., 2014).

Other applications of V2I communication are in traffic signal controllers. Signal controller systems with V2I can send signal timing information to vehicles waiting at or approaching the intersection (Nguyen et al., 2017). Other V2I systems incorporate control algorithms, such as GLOSA, that can recommend vehicle trajectory adjustments so that vehicles arrive at the intersection at the optimal time to reduce delays or fuel consumption (Stebbins et al., 2017).

### 2.1.3. Vehicle to Everything Communication

V2X communication represents the combination of both V2V and V2I communication. Such systems can reduce the bandwidth required for V2I and V2V communication and thus allow data to be transferred more reliably between nodes in the system (Jia and Ngoduy, 2016a). In the network architecture presented in Figure 2.3 by Jia and Ngoduy, V2V communication is used to inform nearby vehicles about their kinematic behavior in order to assist in driving more cooperatively. Meanwhile, V2I communication is used to pass traffic information collected RSUs to upstream vehicles to inform them about upcoming conditions.

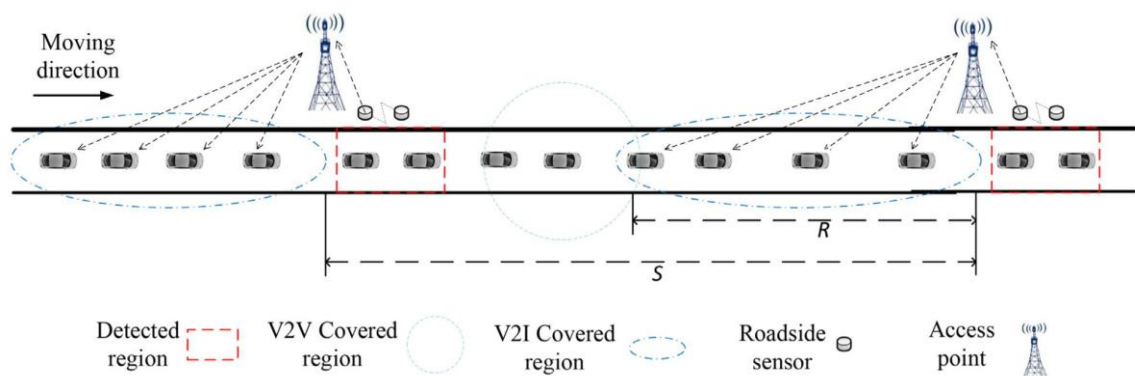


Figure 2.3. V2X communication architecture for improved signal reliability and traffic management. (Jia and Ngoduy, 2016a).

## 2.2. Cooperative Driving

Human drivers tend to exhibit non-cooperative driving behavior. The decisions they make are designed to maximize their own driving benefit regardless of their impact on other drivers (Bagloee et al., 2016). Of course, there are limits to such selfish driving behavior. Some driving maneuvers may provide a benefit but are perceived by the driver to be too risky to attempt, such as changing lanes when a small gap is available. Drivers thus will not always drive to maximize their benefits. There is a limit to the risk drivers are willing to take in order to receive some driving benefit. A smaller benefit or more substantial risk leads to a lower probability a driver will act to improve their situation. This type of behavior is dependent on the type of driver, but it can be considered as a politeness factor (Kesting et al., 2007). A low politeness factor would imply very selfish driving behavior, while a higher politeness factor would equate to more

selfless driving and a willingness to cooperate with other vehicles. However, even if a human driver is willing to cooperate, they often lack the information to provide optimal cooperation.

By leveraging information provided by vehicular communication systems, cooperative driving can improve overall traffic efficiency by providing drivers or AVs with information on driving behavior that is beneficial to multiple drivers rather than only one. The concept of cooperative driving was first proposed in 1966 to determine the feasibility of a high-speed ground transport system in the United States (Levine and Athans, 1966). Control theory was used to develop an algorithm that was able to manage accelerations of platoons of vehicles on a highway-like system so that vehicle speeds and densities could be increased while maintaining overall system stability. Errors in acceleration control among vehicles were also expected under normal operating conditions. As such, the proposed control algorithm was designed to minimize the acceleration errors and their impacts on the stability to determine the optimal platoon size for linear control (i.e., no lane changes were considered). The results showed that up to three vehicles could reliably be controlled in a platoon.

However, beyond the application of using cooperative driving to form platoons, it has also been used for many other purposes. In the following subsections, different cooperative driving algorithms are discussed and grouped based on their application to highway or urban traffic, as this has the most significant impact on traffic properties and, consequently, the goals and approaches of each control algorithm.

### **2.2.1. Highway Cooperation**

The original cooperative driving research by Levine and Athans mentioned above focused on platooning capabilities on a highway-like, high-speed ground transport system. In furthering this research, Athans also proposed a cooperative merging strategy to determine the optimal merging sequence between vehicles of two separate streams (Athans, 1969).

Optimal merging order algorithms for two different vehicle streams have been proposed using various approaches. In the case of Athans, control theory was used, but no formal proof was given that the algorithm would not result in a crash. Further, in order for the optimal merging sequence to be determined, the total number of vehicles to merge as well as their speeds and positions had to be known. However, vehicle counts in traffic streams are measured by flow rates, as vehicles are always arriving from other locations in the network. Exact numbers to perform the optimal merging sequence cannot be known. In addition, vehicle communication architecture to enable information sharing for an optimal merging sequence was not specified.

As a solution to this, Mosebach et al. introduced a decentralized algorithm to allow two streams of vehicles to merge with the least disturbance while also guaranteeing that no collisions would occur (Mosebach et al., 2016). Instead of requiring a complete picture of all the vehicles to be merged, they only considered vehicles that entered a defined control area near the merging point. The algorithm was classified into three phases. First was data collection, where each vehicle that entered the merging area received the time for the preceding vehicle to complete

the merging maneuver. The data transmission between vehicles was designed to be light-weight to minimize communication overhead. The second phase was the deceleration phase, where vehicles that entered the merging area decelerated at rates determined by the algorithm. The deceleration continued until no collision with the preceding merging vehicle was guaranteed. The third phase was the acceleration phase. Once the vehicle was guaranteed not to have a collision with the preceding vehicle in the merged stream, it accelerated to leave the merging area at a certain speed, as shown in Figure 2.4. As a result of the deceleration, however, the impact on upstream vehicles became more pronounced with an increasing number of vehicles in the stream. With 40 vehicles simulated in each traffic stream, jam conditions began to form after only 15 vehicles from each stream entered the control area.

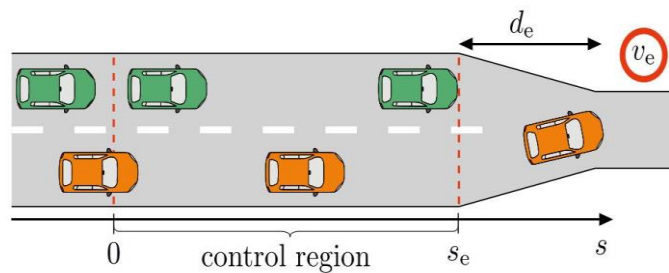


Figure 2.4. Merging control of two streams of cooperative vehicles, where  $s_e$  is the start point for merging,  $d_e$  is the length available for merging, and  $v_e$  is the required exit velocity (Mosebach et al., 2016).

A centralized control algorithm has also been explored for the highway merging scenario. Vehicles that enter the cooperative area receive trajectories of other vehicles within the control area to coordinate smooth lane changes as the vehicles approach the fixed merging point (Ntousakis et al., 2016). Here, a single lane highway is used as the merging lane, and vehicles adjust their accelerations based on the centralized system controller. A cost function for minimizing traffic disturbances is presented as the weighted sum of squares of the acceleration, jerk, and derivative of jerk, helping to provide higher passenger comfort and less engine work for cooperative merging.

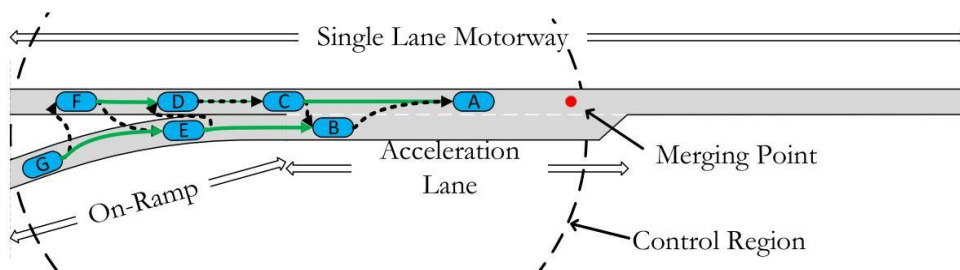


Figure 2.5. Centralized control algorithm for merging streams on a highway. The green arrow indicates the current leader, and the black arrow indicates the planned leader after merging (Ntousakis et al., 2016).

While cooperative merging has been shown to smoothly enable lane changes with improved traffic stability, different penetration rates of connected vehicles can lead to different results on how the traffic is improved (Talebpour and Mahmassani, 2016). The study by Talebpour and Mahmassani analyzed different penetration rates of connected vehicles equipped with automatic cruise control (CACC) for merging onto a single lane highway. A gap-acceptance based model was used to simulate the lane changing behaviors of the merging vehicles. Results showed that increasing penetration rates of connected vehicles resulted in increased throughput of the highway, and with at least 90% connected vehicle network penetration, there is no traffic flow breakdown caused by merging vehicles from the entry ramp.

The studies discussed above only look at scenarios where vehicles merge into a single lane. Major highway systems typically have multiple lanes, which can change how the highway absorbs new vehicles and how cooperative vehicles can react to accommodate merging vehicles streams. Van Arem et al. studied the impact of a highway lane reduction from four to three lanes for different market penetrations of connected vehicles (van Arem et al., 2006). According to the results, connected vehicle penetration below 40% did not show any significant impacts on traffic performance, but increasing penetration beyond this point led to increasingly more efficient traffic.

Xiao et al. also studied the effects of vehicles with CACC on a multilane highway lane reduction scenario. They focused on how switching between automatic cruise control and human driving can affect traffic flow at bottlenecks (Xiao et al., 2018). Connected vehicle penetration below 40% only showed minor improvements, which is in line with findings from van Arem et al. It was not until at least 60% penetration when traffic flow and merging capacity at the bottleneck showed significant increases in performance. However, the CACC of connected vehicles was deactivated for vehicles approaching the bottleneck due to increased traffic density and the necessity for lane changes. This reduces the potential performance of a system equipped with vehicle communication technologies.

Cooperative control algorithms summarized above use either CACCs or a unique algorithm to manage vehicle lane-changing maneuvers. And while the algorithms that utilize original control manage cooperative acceleration more proactively than CACCs, particularly for centralized algorithms, these do not factor in lane changes on multilane highways. As VROW can only operate on multilane roads, the single lane merging algorithms are not compatible with the VROW algorithm. Furthermore, these algorithms all use a single static merging point to determine an optimal merging strategy. This makes sense for a single lane highway situation because the most critical disturbance to traffic comes from the entrance ramp. However, when VROW sends a lane-change request, no single merging point for vehicles can be identified.

CACCs can help to smooth overall traffic flow and manage disturbances caused by the lane changes and can support multilane scenarios, but they do not proactively adjust acceleration to create a gap for a merging vehicle unless provided information by a higher-level control system designed for cooperative merging. Instead, CACCs only consider the preceding vehicle

and any other traffic information received from downstream vehicles to smooth the traffic flow. In the case of VROW lane changes, a gap needs to be proactively created if one is not readily available.

### 2.2.2. Urban Roadway Cooperation

Much of the literature regarding driving control algorithms in urban settings involves some form of eco-driving or green light arrival optimization. These types of algorithms focus on individual vehicles, not cooperation amongst them. There are, however, several algorithms for urban cooperative driving.

Zhao et al. proposed the use of connected autonomous vehicles (CAVs) to become platoon leaders that assist human-driven vehicles in driving with higher fuel efficiency when approaching a signalized intersection (Zhao et al., 2018). CAVs receive the signal timing information from the downstream traffic controller and respond accordingly to minimize fuel consumption. Human-driven vehicles traveling behind the CAVs form a platoon and pass through the intersection with the optimal trajectory. The cooperative algorithm also considered the lead vehicle's impact on the following vehicles and attempted to find the trajectory that benefits the group over any specific vehicle in the platoon. Stebbins et al. also applied a similar approach but did not incorporate the consideration of lead vehicles to optimize the entire platoon (Stebbins et al., 2017).

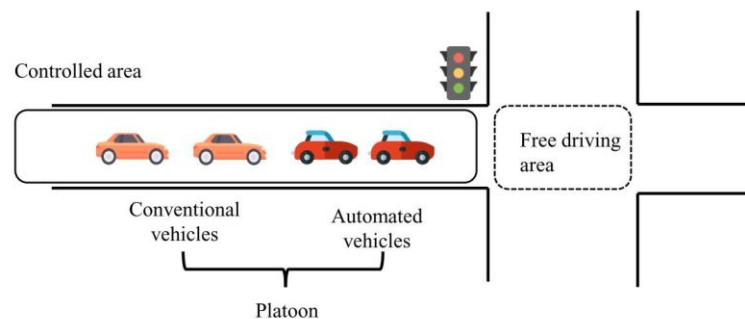


Figure 2.6. Platoon-based cooperative eco-driving with AVs as leaders (Zhao et al., 2018)

Cooperative urban driving strategies mainly seek to optimize an objective such as travel time or fuel-efficiency. Lane changing is not considered. In addition, the utilization of signal speed advisory algorithms creates platoons, forming a denser traffic condition and smaller gaps as a consequence. Vehicles that need to change lanes are thus unable to do so in platoons formed by these types of control algorithms. A cooperative driving algorithm that has incorporated cooperative lane changes for urban roads has been proposed by Atagoziyev et al. Different lane-changing cases have been defined to describe the situations a vehicle may encounter when attempting to change lanes (Atagoziyev et al., 2016). Based on the location of the surrounding vehicles, either the vehicle attempting the lane change or one of the surrounding vehicles will respond to enable smooth lane changes. The algorithm can also be applied to multiple vehicles that requiring such mandatory lane changes in any lane, creating a lane

change scheduling effect that ensure all vehicles will be able to change lanes when reaching the merging point. This algorithm can also be applied to both highway and urban roads. But in the simulated scenario with six lane-changing and four lane-keeping vehicles, the algorithm took 30 seconds for all vehicles to complete their lane change. The time for vehicles to complete their lane changes, however, may be too short for practical application with VROW. On an arterial road, many vehicles will be requested to change lanes, and the algorithm may fail to create enough gaps before buses are delayed by preceding vehicles.

### 2.2.3. Acceleration and Jerk as Safety and Comfort Parameters

Connected vehicles are driven by humans but receive information regarding their surroundings and suggested acceleration values to improve the overall traffic flow. If human drivers are expected to follow the recommended acceleration, the new value must be within a reasonable range and reasonably close to the vehicle's current acceleration. Having an algorithm that limits these vehicle dynamics within a certain range would significantly improve the safety and comfort of drivers and passengers as well as their likelihood to follow the suggested acceleration control (Moon and Yi, 2008; Svensson and Eriksson, 2015).

Jerk [ $\text{m/s}^3$ ] is the temporal derivative of acceleration and defined the rate at which acceleration changes (Schot, 1978). Large jerk values indicate that the acceleration changes quickly, while smaller values mean that acceleration is changing more slowly. Jerk also does not need to keep the same sign as acceleration. A positive acceleration but negative jerk means that the rate of acceleration is increasing at a slower rate. If the negative jerk is applied long enough, the positive acceleration will eventually turn to zero and then become negative at an increasing rate. Jerk enables the smooth transition between positive and negative acceleration, which is particularly helpful in controlling vehicle dynamics (Bae et al., 2019). Particularly when applied to cooperative control algorithms that adjust vehicle accelerations, jerk can be used to determine a suitable new acceleration value that maintains driver comfort.

The consideration of jerk as a comfort indicator has been widely applied to research involving vehicle control algorithms, some of which were mentioned in section 2.1.2. However, the acceptable range for jerk has some differences in the literature. Elbanhawi et al. used an absolute maximum jerk of  $0.6 \text{ m/s}^3$  as a constraint for acceleration changes to improve passenger comfort in AVs (Elbanhawi et al., 2015). A much larger absolute jerk value of  $4 \text{ m/s}^3$  has also been applied for cooperative eco-driving with autonomous vehicles (Zhao et al., 2018). Svensson and Eriksson showed that a maximum jerk to provide a high comfort level for AVs was  $0.9 \text{ m/s}^3$  (Svensson and Eriksson, 2015). Providing even smoother control and higher comfort, Ntousakis et al. controlled vehicle dynamics one step further by minimizing the derivative of jerk, also known as jounce (Ntousakis et al., 2016).

The acceptable range for acceleration is more agreed upon than that for jerk. For normal braking, acceleration for human drivers is typically  $-2.0 \text{ m/s}^2$  but can reach as low as  $-5.0 \text{ m/s}^2$  (Moon and Yi, 2008; Paolo B. et al., 2014). At the opposite end of the acceleration range,  $3.0$

m/s<sup>2</sup> is generally accepted for normal (i.e., non-aggressive) driving behavior (Moon and Yi, 2008).

## 2.3. Driving Behavior Models

Driving behavior models can be broken down into car-following and lane-changing models. The car-following models only focus on the longitudinal control of the vehicle, while lane-changing models concentrate on modeling the behavior in situations where a driver would change lanes to improve their driving situation based on different behavioral parameters. On single-lane roads, using only a car-following model is enough to accurately represent vehicle interactions. However, car-following and lane-changing models must be integrated in order to fully represent complete driving behavior on multi-lane roads. Driving behavior models typically try to replicate human driving behavior, but increasing research is focused on adapting these models or on creating new ones to model connected or autonomous vehicles.

### 2.3.1. Car-Following Models

Gazis et al. were one of the first to propose a car-following model, where the acceleration of the vehicle is proportional to the relative velocity and distance of the preceding vehicle (Gazis et al., 1959). Gipps introduced additional constraints to the car-following model, such as a maximum and minimum acceleration, vehicle length, and desired speed, so that the parameters and behavior more accurately resembled real-world behavior (Gipps, 1981).

There have been many other car-following models that have been defined, such as the optimal-velocity model by Bando et al. and the generalized force model by Helbing and Tilch (Bando et al., 1995; Helbing and Tilch, 1998). One of the most frequently used car-following models, the Intelligent Driver Model (IDM), was developed to address the unrealistic acceleration, following gap, and reaction time parameters in previous models (Treiber et al., 2000). IDM enables the ego vehicle to freely accelerate to a desired speed should there be no preceding vehicle present to limit this acceleration. Upon approaching a preceding vehicle, the ego vehicle applies a braking force proportional to its approach velocity and distance to the preceding vehicle. The IDM is summarized in equation 2.1 below (Treiber et al., 2000).

$$\dot{v}_\alpha = a^{(\alpha)} \left[ 1 - \left( \frac{v_\alpha}{v_0^{(\alpha)}} \right)^\delta - \left( \frac{s^*(v_\alpha, \Delta v_\alpha)}{s_\alpha} \right)^2 \right] \quad (2.1)$$

Equation 2.1 calculates the vehicle's acceleration ( $\dot{v}_\alpha$ ), which is a function of the vehicle's current acceleration ( $a^{(\alpha)}$ ), velocity ( $v_\alpha$ ), desired velocity ( $v_0$ ), the desired minimum gap ( $s^*$ ) and the actual gap to the preceding vehicle ( $s_\alpha$ ). The alpha symbol ( $\alpha$ ) denotes that the term applies to the ego vehicle. A term with  $\alpha - 1$  would indicate that it refers to the relevant value of the preceding vehicle. For example, the preceding vehicle's velocity would be indicated by  $v_{\alpha-1}$ . The  $\delta$  term is known as the acceleration exponent, which describes how the acceleration decreases when approaching the desired velocity.

The desired minimum gap is described by equation 2.2:

$$s^*(v, \Delta v) = s_0^{(\alpha)} + s_1^{(\alpha)} \sqrt{\frac{v}{v_0^{(\alpha)}}} + T^\alpha v + \frac{v\Delta v}{2\sqrt{a^{(\alpha)}b^{(\alpha)}}} \quad (2.2)$$

where  $v$  is the ego vehicle's velocity,  $\Delta v$  is the relative velocity between the ego and preceding vehicles,  $s_0$  and  $s_1$  are respectively the additive and multiplicative parts of the minimum desired distance,  $T$  represents the safe time headway,  $a$  represents the maximum acceleration, and  $b$  is the desired deceleration. Equation 2.2 provides a more realistic car following behavior for different traffic conditions, as it is based on both velocity and headway to the preceding vehicle. If the distance to the preceding vehicle is greater than the minimum desired distance, the vehicle accelerates at a rate depending on the ratio of the desired and actual distance, as seen in equation 2.1. The realistic behavior described by the IDM has also led to its application in modeling connected vehicles to determine how vehicle communication can affect string stability and flow rates (Talebpoor and Mahmassani, 2016).

### 2.3.2. Lane-Changing Models

As with car-following models, there are many different types of lane-changing models. In replicating lane-changing behavior, the process can be divided into three different levels: operational, which controls the vehicle and executes lane changes; tactical, where the different lane change options are evaluated based on some criteria and plans a trajectory; and strategic, which decides if a lane change is to be performed (Salvucci, 2002). The lane-changing models can also be classified into four groups, which are rule-based, discrete choice-based, artificial intelligence-based, and incentive-based models (Rahman et al., 2013).

Rule-based lane-changing models only execute a lane change once certain conditions are met. These models are simple and thus require less computational effort, but there are also difficulties in calibrating the parameters, and they do not consider different gap acceptance variability from drivers (Rahman et al., 2013). Gipps' developed such a rule-based model for lane-changing that is based on available gaps and the speed advantage gained from performing a lane change, which also integrated with his car-following model by limiting vehicle accelerations to perform lane changes (Gipps, 1986). Other models, such as Ahmed's or Toledo et al.'s discrete choice-based models, use logit or probit models to determine a probability of lane change occurring based on the velocities of the lead and lag vehicles in the target lane (Ahmed et al., 1996; Toledo et al., 2003). Artificial intelligence models utilize machine learning techniques such as fuzzy logic or artificial neural networks to understand how drivers behave under certain conditions. Artificial neural networks, in particular, are able to accurately reproduce lane-changing behavior, but vast datasets are needed to produce such models (Hunt and Lyons, 1994). This can be a major limitation, as lane-changing data is challenging to collect. Additionally, the validation of artificial intelligence models is not easy because the parameters used by these complex algorithms often have no real-world interpretation (Rahman et al., 2013).

The final type of lane-changing model, incentive-based models, operate by encouraging lane changes based on a utility function or lane change desire for lane attractiveness, while also limiting lane changes based on the acceleration change required and safety when changing lanes (Kesting et al., 2007; Schakel et al., 2012). The Minimizing Overall Braking Induced by Lane Change (MOBIL) model developed by Kesting et al. is an example of an incentive-based model and was designed to work with the IDM car-following model. The incentive criterion is based on acceleration differences between lanes and activates a lane change should this difference exceed a threshold (Kesting et al., 2007). Equation 2.3 shows the basis of the incentive model.

$$\bar{a}_c - a_c + p(\bar{a}_n - a_n + \bar{a}_o - a_o) > \Delta a_{th} \quad (2.3)$$

In the inequality above, each term with the “bar” notation indicates the new acceleration after a lane change occurs. The  $a_c$  terms are the acceleration of the ego vehicle (i.e., the driver considering a lane change). The new and old followers are represented by  $a_n$  and  $a_o$ , respectively. A politeness factor  $p$  is also included, which takes values between 0 (no politeness) and 1 (maximum politeness). A threshold of  $\Delta a_{th}$  is also defined so that acceleration benefits from changing lanes do not enable lane changes for minor improvements.

The introduction of a politeness factor made it possible to model different driving behaviors within the same network. Not all vehicles act precisely the same or accept the same gap when looking to change lanes. The politeness factor can be thought of as a degree of passive cooperativeness among the drivers, as less disruptive lane changes will occur with higher politeness factor values (Kesting et al., 2007). However, the MOBIL model only represents the operational layer of the lane-changing process. As such, vehicles will not behave differently for mandatory versus discretionary lane changes.

### 2.3.3. Vissim’s Driving Behavior Model

As a microscopic traffic simulator, Vissim’s driving behavior model is composed of both car-following and lane-changing models. In an urban environment, a car-following model known as Wiedemann 74 is applied, but for highway simulation, the Wiedemann 99 model is used instead. While there are different car-following models for urban roads and highways, the lane-changing model in Vissim is the same for both situations with only different default values set for certain parameters. The remainder of this section will review the theory behind the Wiedemann 74 car-following model and Vissim’s lane-changing model. As the modeling in Vissim for this research was done with urban roads, the Wiedemann 99 model will not be mentioned here. It should also be noted that although the Wiedemann models are used in Vissim, there have been modifications made to the original models by PTV Group that are unknown to the public (Olstam and Tapani, 2004). However, detailed workings of the Wiedemann models that are used in Vissim have been provided in the PTV Vissim User Manual (PTV Group, 2018).

### The Car-Following Model

The Wiedemann 74 car-following model is a psychophysical model that has identified five different regimes of car-following behavior (Wiedemann, 1974). The driving behavior changes when a vehicle crosses between regime thresholds. Figure 2.7 shows the orientation of the different regimes as a function of velocity change and distance from the preceding vehicle.

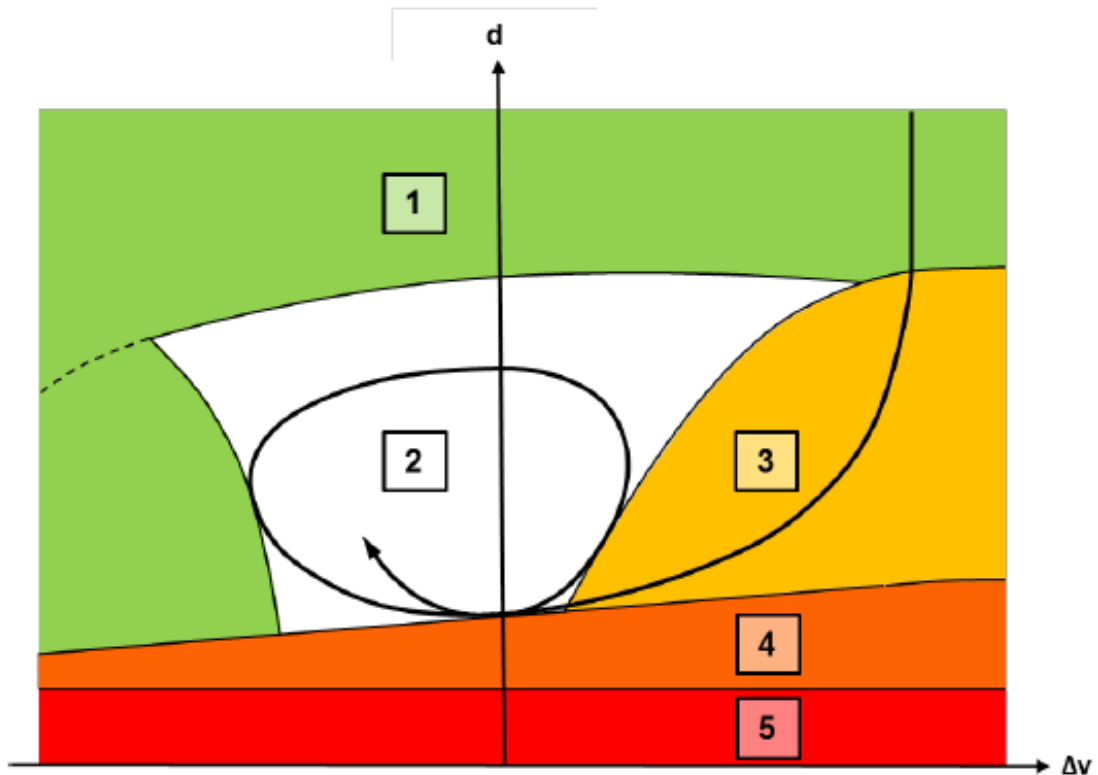


Figure 2.7. The Wiedemann 74 model's five regimes for car-following behavior (PTV Group, 2018). The behavior corresponding to each regime is mentioned in the text.

Referencing Figure 2.7, a description of the driving behaviors in different regions is provided. The first regime is the free-flow traffic state. Here, vehicles are free to reach their desired speed and travel without any impedance. The second regime is the following state. Vehicles in this state are free to move within this area. This represents the small vehicle control errors of human drivers in an urban context, as a human driver that approaches a preceding vehicle will continue to do so up to a certain point depending on their desired safety distance, represented by the threshold between regions two, three, and four. After this point is reached, the human driver will reduce their speed to attempt to match the preceding vehicle. However, because of the imperfect control abilities of human drivers, this initial speed adjustment introduces some error, and the vehicle falls back to the border of the car-following regime and free-flow regime. This process repeats itself until one of the vehicles changes lanes. The third regime is known as the approaching state, which is the transition between the free-flow state and the following state. A human driver in this state approaches a preceding vehicle until a certain distance, where they then brake to fall into the following state. The fourth regime is the braking state.

This is where human drivers exceed their minimum desired distance to the preceding vehicle and adjust their speed. The final state represents the collision state. If no braking action is taken as the ego vehicle approaches the preceding vehicle, a collision will occur. In Vissim, this does not happen unless unstable car-following parameters are chosen.

The Wiedemann 74 model is governed by a desired safety distance, defined by:

$$d = ax + bx \quad (2.4)$$

where  $ax$  is the standstill distance between the ego and preceding vehicles. The desired safety distance also varies as a function of the vehicle's velocity, represented as  $bx$  and defined by equation 2.5.

$$bx = (bx_{add} + z * bx_{mult})\sqrt{v} \quad (2.5)$$

The  $bx_{add}$  term is the additive safety distance factor. Increasing this term will lead to larger following distances as speed increases. The variability of driving behaviors and desired following distances are represented by  $z$ , which is a normal distribution with a range of [0,1], a mean of 0.5, and a standard deviation of 0.15. Each vehicle is assigned a value for  $z$  based on the distribution. The  $bx_{mult}$  term is the multiplicative safety distance factor. As this term is multiplied by  $z$ , larger  $bx_{mult}$  values result in larger variabilities in the desired safety distance. Lastly is the velocity term,  $v$ , which changes the desired safety distance as vehicle speed changes. The square root function of velocity implies that changes in velocity at lower speeds result in greater changes in desired safety distance. Only  $bx_{add}$  and  $bx_{mult}$  can be changed to calculate  $bx$ . Because these values impact the desired safety distance, they ultimately impact the saturation flow rate (Park and Qi, 2005).

Once the desired safety distance has been defined, the simulation can determine appropriate actions for the vehicle based on the driving regime the vehicle is currently in (PTV Group, 2018). If the preceding vehicle's distance is greater than or equal to 110% of the desired safety distance, the ego vehicle is in the free-flow regime. At a front vehicle distance between 100% and 110% of the desired safety distance, the vehicle enters the approaching state. When the preceding vehicle's distance is equal to the desired safety distance (i.e., 100%), the vehicle is in the car-following state and matches the speed of the preceding vehicle. Any time the safety distance is greater than the distance to the preceding vehicle, the vehicle is in the braking regime. The car-following model also includes a safety distance reduction factor. When vehicles are within a set distance to the traffic signal (default value of 100 meters), the desired safety distance is reduced by 40% (default value) to simulate higher driver attention levels when approaching intersections.

### **The Lane-Changing Model**

Vissim enables the modeling of multi-lane road segments and has thus incorporated a lane-changing model into the software. This model was developed by Sparmann as a rule-based model that depends on the gap size and relative speeds of the lead and lag vehicles in the

desired lane (PTV Group, 2018; Sparmann, 1978). The lane-changing model classifies lane changes as either necessary or free lane changes.

Free lane changes are performed to increase the vehicle's distances to their leading and trailing vehicles and to achieve a higher speed. They can only occur when the trailing vehicle's safety distance, which is based on the velocity difference between the two vehicles, is less than or equal to the proposed distance to the new lead vehicle. Necessary lane changes are performed in order for the vehicle to merge into the correct lane to continue on its route. Necessary lane changes are intended to be more aggressive than free lane changes, and the lane-changing vehicle is allowed to force the following vehicle in the new lane to decelerate, provided that the forced deceleration on the trailing vehicle does not exceed a set threshold. The lane-changing threshold also includes a safety distance reduction factor similar to that used in the car-following model. The desired safety distance is again reduced by 40% to account for heightened attentiveness of the driver when changing lanes.

### Cooperative Lane-Changing

Vissim also includes some parameters to define cooperative lane-changing behavior. This encourages vehicles that are preventing a free or necessary lane change to create a gap in their lane by changing their own lane (PTV Group, 2018). Referencing Figure 2.8, Vehicle B wants to change from the rightmost lane to the center lane. Vehicle A is informed by Vehicle B's turning signal of the lane change and proceeds to create a gap by changing into its left lane. Vehicle A can perform this maneuver if the braking action by Vehicle C is in line with the requirements of a necessary lane change. Additionally, the cooperative lane change can only occur if the new lane allows Vehicle A to continue on its route, Vehicles A and B have a low relative velocity, and the collision time (i.e., the time for the Vehicle A to catch up to Vehicle B) is greater than 10 seconds (PTV Group, 2018). While this can quickly create a gap to accommodate a lane change from the VROW lane, there is no way in Vissim to turn this parameter on only when a VROW bus is present. This made the cooperative lane-changing parameter unsuitable for the cooperative driving application.

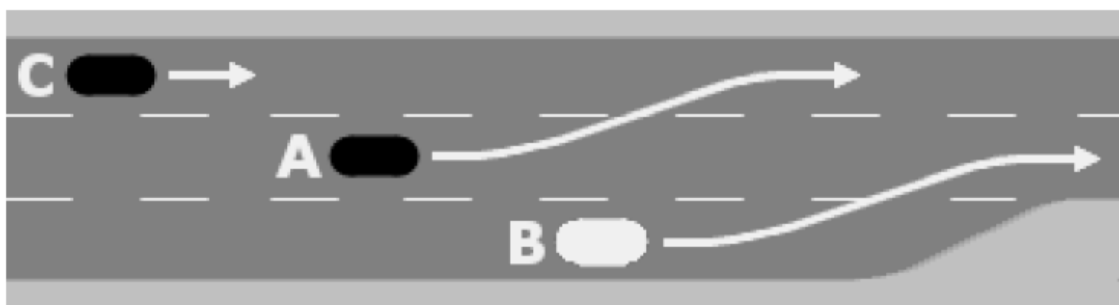


Figure 2.8. Schematic of cooperative driving in Vissim (PTV Group, 2018).

## 2.4. Virtual Right of Way

Virtual Right of Way is a dynamic and on-demand system that provides public transport vehicles with spatial and temporal priority for faster and more reliable operations (Xie et al., 2019). VROW relies on V2X communication technology to clear its lane of downstream vehicles that are expected to delay its operation, thus creating a dynamic bus lane that is only activated for vehicles that will delay public transport operations.

The advantages of VROW are most apparent in comparison to other bus lane prioritization methods. Traditionally, bus priority lanes are created in the form of permanent bus lanes, which provide a dedicated lane for buses at the expense of general traffic. While this measure may work well on roads with a high bus frequency, applying permanent bus lanes to roads with a low bus frequency results in a loss of road capacity by a lane that is frequently empty (Rau et al., 2019). Other methods such as the Intermittent Bus Lane (IBL) and Bus Lanes with Intermittent Priority (BLIP) have been proposed as a means of providing a better balance of the use of road space between private and public vehicles (Eichler and Daganzo, 2006; Viegas and Lu, 2000). However, both of these priority measures are limited in optimally clearing vehicles in front of the bus. The IBL technique only prevents vehicles from entering the bus lane but does not require vehicles already in the bus lane to change lane (Viegas and Lu, 2000). BLIP operates more optimally by requesting vehicles within a fixed distance in front of the bus to change lanes (Eichler and Daganzo, 2006).

VROW addresses the issue of suboptimal dynamic bus lane performance by predicting which vehicles will delay the bus operation and sending them a signal to change lanes (Xie et al., 2019). For VROW to do this, however, it requires information on signal controller timings via V2I communication as well as distance and velocity information for the vehicles and buses through V2X communication. With this data, the vehicles downstream of the bus determine the time for the bus to catch up to them by comparing the distance and relative velocity between the bus and the vehicles. If the bus catches up to one of the vehicles before the vehicle passes through the traffic signal, or if the traffic signal will turn red before the vehicle passes through it, the vehicle will be requested to change lanes. Exceptions are allowed for vehicles that need the bus lane to make a turning movement and for vehicles that cannot change lanes due to an insufficient gap in the adjacent lane.

The result is a more flexible bus priority system that only requests vehicles to change lanes if it is very probable that they will hinder the performance of the bus. This reduces the number of lane changes out of the bus lane when compared to BLIP and therefore leads to less disturbance on the general traffic. The incorporation of signal timing data to determine delays also aids in improving the buses' performance, as vehicles can avoid queueing in front of the bus while stopped in a red phase. This was something that other bus lane priority measures struggled with. The setback length before the intersection was fixed, thus ending the priority lane near the intersection previously allowed vehicles to queue ahead of the bus.

Despite these improvements, however, it is still not known how vehicles will be able to successfully merge into the adjacent lane if no acceptable gaps are available. In urban traffic conditions, particularly during peak hours, finding safe gaps to perform these maneuvers can be challenging. Additionally, the performance of VROW relies heavily on the cooperation of vehicles downstream of the bus to comply with the lane-changing signal. As human drivers tend to drive in a way to maximize their own benefit, it is not clear what the impact of various non-compliance rates would be on the system's performance.

### 3. Chapter 3: Methodology

The proposed cooperative driving algorithm is designed to integrate into VROW operations and can thus be thought of as an extension to the VROW algorithm. VROW requires the cooperation of downstream vehicles in its lane to change lanes when requested. The cooperative driving algorithm introduces three new cooperative behaviors to assist in lane changing, which are depicted in Figure 3.1.

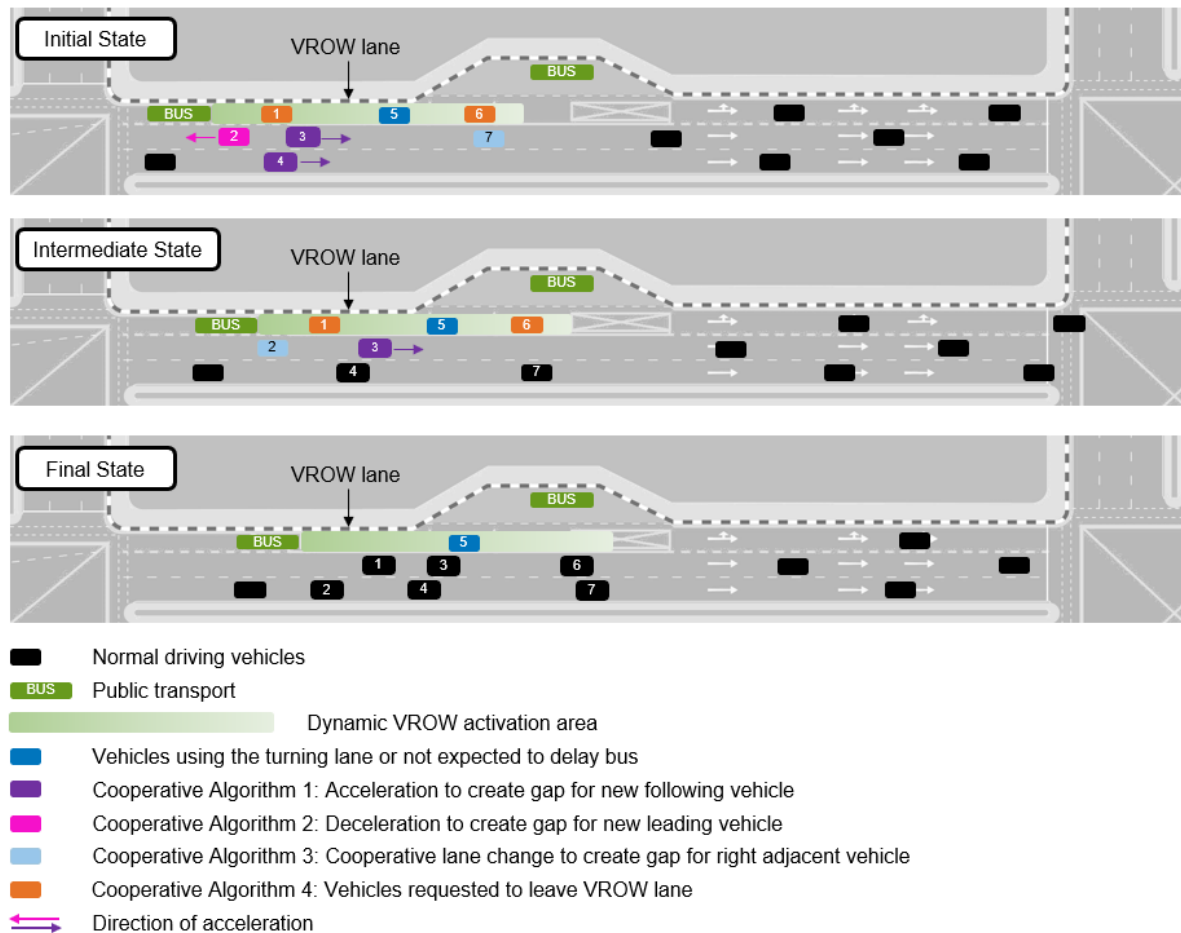


Figure 3.1. Conceptual operation of VROW with cooperative driving.

In the figure above, a VROW bus is traveling on the leftmost lane with a particular dynamic clearing distance. Vehicles 1 and 6 receive a signal to change lanes to provide priority for the bus. Vehicle 5, however, is not requested to change lanes. There are two cases for this outcome. Either the vehicle is using the leftmost lane to complete a turning movement at the intersection, or it is traveling with a trajectory that will not delay the bus's operation. In the initial state, vehicles 1 and 6 are unable to change lanes due to insufficient gap sizes in their adjacent lanes. The VROW algorithm without any cooperative driving behavior from vehicles in the adjacent lanes would perform poorly, as vehicles in the VROW lane would not be able to safely change into their adjacent lane.

For the situations where vehicles in the VROW lane are unable to perform a lane change, the cooperative driving algorithm is designed to make this possible. The fastest way to create a gap is by performing a cooperative lane change, which is denoted Cooperative Algorithm 3 and represented by vehicle 7 changing from the middle to rightmost lane, thus providing space for vehicle 6 to change lanes. While this is the preferred response to support VROW, a cooperative lane change is not always possible. Perhaps there is no gap available in the right adjacent lane, the lane does not allow the necessary turning movement for the vehicle as it approaches the intersection, or there is no lane physically available to support the maneuver. In these cases, vehicles will then default to adjusting their acceleration to create a gap. This acceleration behavior is categorized as either Cooperative Algorithm 1 or 2, depending on the relative location of the vehicle requesting to change lanes from the VROW lane. In Figure 3.1, vehicle 3 executes Cooperative Driving Algorithm 1, as it is in front of the vehicle requesting to merge. Vehicle 2 executes Cooperative Driving Algorithm 2 because it is behind the point where vehicle 6 would like to merge.

Notice that vehicle 4 also receives some instructions for cooperative driving even though it is not directly adjacent to the merging vehicle from the VROW lane. In the ideal case, vehicles 2 and 3 would change lanes to accommodate vehicle 1 in changing lanes. But as the gap is not available for these two vehicles, they can only adjust their acceleration. Vehicle 4 receives the information about the merging maneuver request for vehicle 1 via multi-hop and tries to accommodate a lane change for vehicles 2 and 3. Both of these vehicles are seeking to change lanes, but vehicle 4 can only create a gap in front or behind itself by changing its acceleration. Because vehicle 2 is closest to the bus's position, it is given priority in changing lanes, and vehicle 4 accelerates in response. Creating gaps closest to the bus will always be given the highest priority for merging because the areas closest to the bus are the most critical in delaying it. A summary of the different functions of the cooperative driving algorithm is provided in Table 3.1, and the exact details of how the cooperative driving algorithm works will be discussed later in this chapter.

Table 3.1. Summary of cooperative driving algorithm functions.

Cooperative Algorithm	Resulting Driving Behavior
1	Acceleration changes to accommodate left preceding vehicle's lane change request
2	Acceleration changes to accommodate left following vehicle's lane change request
3	Cooperative lane change in the non-VROW lane to provide a gap for a vehicle in the VROW lane that is requesting a lane change
4	Lane change of vehicle in the VROW lane to the right adjacent lane

### 3.1. Cooperative Driving Integration with VROW

The original VROW algorithm presented by Xie focused on the development of a dynamic clearing distance for VROW that can predict if vehicles will delay the bus's operation (Xie et al., 2019). The exact mechanisms used were discussed in section 2.4. The main focus of this was on the vehicles in the VROW lane. Vehicles in non-VROW lanes also received information about the presence of a bus. However, they only supported VROW by not entering its lane unless they needed the lane for a turning movement or if they would not delay the bus.

In order to integrate cooperative driving with VROW, a communication architecture needed to be defined. The architecture, depicted in Figure 3.2, keeps much of the communication links of the original VROW algorithm. V2X communication was used to inform vehicles in the VROW lane about VROW bus data as well as signal timing information. VROW information was also passed to vehicles in non-VROW lanes to inform them not to enter the bus's lane. In the original VROW algorithm, however, non-VROW lane vehicles also received signal timing information. This information allowed them to enter into the VROW lane if they were not expected to delay the operation of the bus. This communication link was removed for cooperative driving to limit unnecessary lane changes and to shift all traffic farther right to create gaps when possible. Non-VROW lane vehicles thus can only enter the VROW lane if they require that lane for continuing on their route.

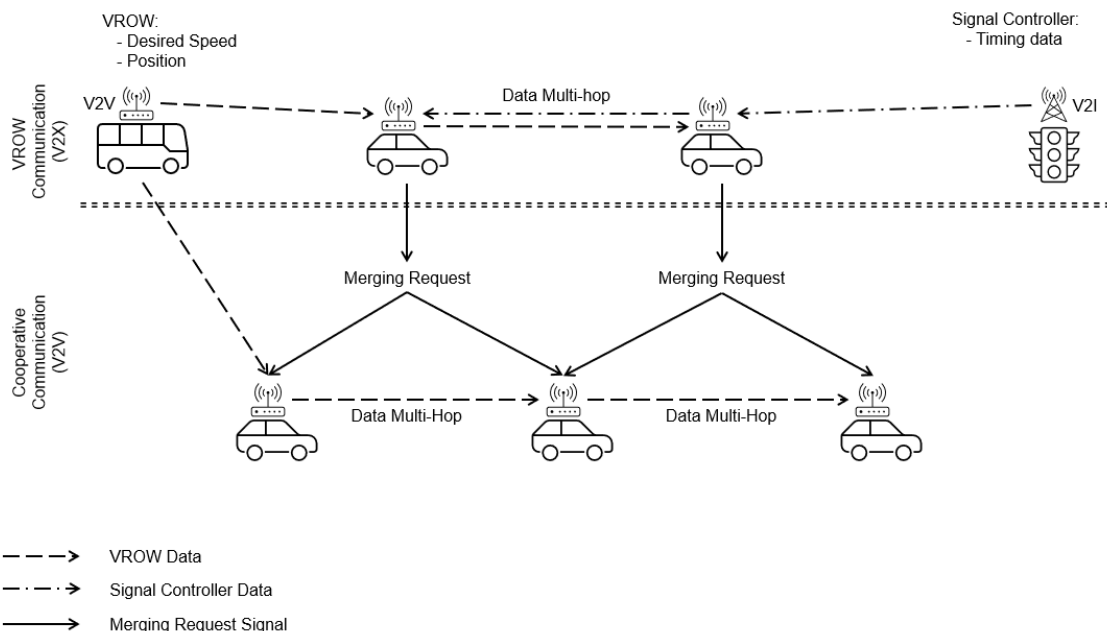


Figure 3.2. VROW and Cooperative Driving Communication Architecture

While the VROW communication architecture remained mostly unchanged, the behaviors of vehicles executing VROW requests had more alterations. Vehicles that were not in the VROW lane had the most changes from the original VROW algorithm, as this was where cooperative driving was implemented. However, much of the core behavior defined for vehicles in the VROW lane did not change. Only the gap acceptance parameters for merging were modified, which is now based on the desired safety distance of the Wiedemann 74 model (equation 2.4) and the safety distance reduction factors. This is discussed in detail in section 3.2.1.

The full control logic for the integration of cooperative driving with VROW is presented in Figure 3.3. As mentioned, the algorithm is only activated when a bus is present and within range. Vehicles receive information regarding the buses desired speed level and current lane. A vehicle on the same lane as the bus, referred to as vehicle A for clarity, determines if the bus will catch up to itself based on its velocity and the bus's desired velocity. Vehicle A receives signal timing information to determine its own amount of time to pass through the intersection. If vehicle A can pass through the intersection before the bus can catch up to the vehicle or before the signal turns red, vehicle A will not delay the bus's operation and does not need to change lanes. No changes are thus made to vehicle A's driving behavior. However, if Vehicle A is expected to delay the bus's operation, a VROW lane change request will be called.

Before a lane change request can be fulfilled, several conditions must be met to ensure a safe lane-changing maneuver. Firstly, if vehicle A is in a queue, it is unable to change lanes. The vehicle must also be in a lane that allows its desired turning movement. If its current lane does not allow the vehicle to follow its route, it does not need to comply with VROW and should proceed to find a lane that allows it to continue on its route. If vehicle A is not in a queue and in a lane that allows its movement, it also needs to check that the right adjacent lane allows its desired turning movement, as this is the lane it will change to by complying with VROW. Lastly, vehicle A must check the available gap in its right adjacent lane before performing a lane-change maneuver. If the gap is acceptable, vehicle A will change lanes, denoted as Cooperative Driving Algorithm 4, and represented by vehicles 1 and 6 in Figure 3.1. On the other hand, if vehicle A cannot find a suitable gap in the right adjacent lane, it is allowed to stay in the VROW lane until a gap is available. During this time, vehicle A sends a merging request signal to the leading and following vehicles in its right adjacent lane. Section 3.2 contains further information regarding the gap acceptance calculation for merging.

Vehicle A relies on a gap between vehicles in its adjacent lane. Again, for clarity, vehicle B will represent the leading vehicle on the adjacent lane, and vehicle C will be the trailing vehicle on the adjacent lane. Vehicles B and C are not on the VROW lane. If a bus is detected, these vehicles need to perform similar initial checks as vehicle A. If they are currently in a queue, they cannot change lanes. They also must find their correct turning lane. If their only turning lane is the VROW lane, they are allowed to enter this lane. Vehicles in non-VROW lanes that are already in their correct turning lanes must keep to their current lane unless directed. Once in their correct turning lane, vehicles B and C can only change their lane if vehicle A requests a lane change as a result of an insufficient gap for merging.

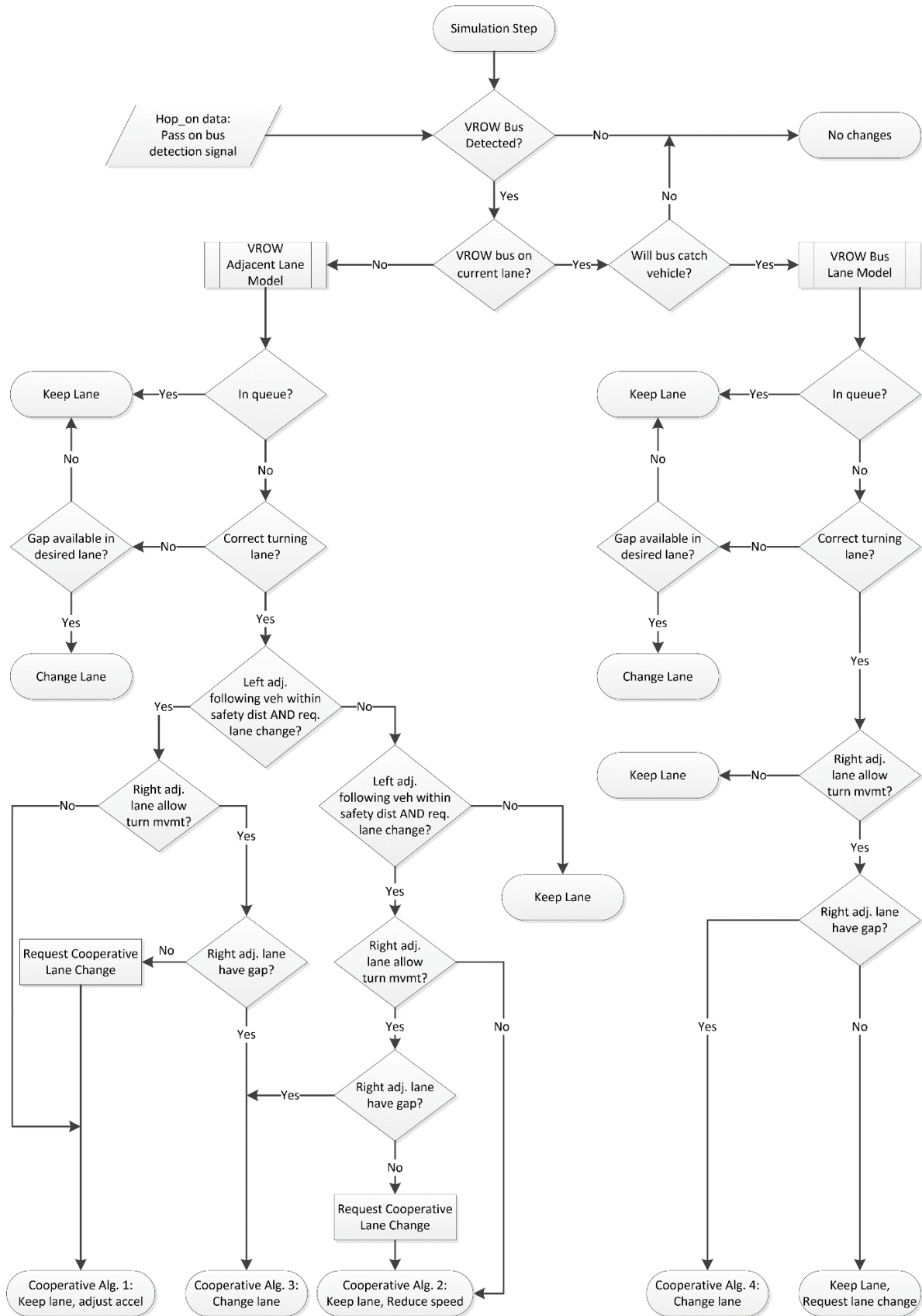


Figure 3.3. Modified VROW algorithm, based on Xie et al. (2019), to incorporate cooperative driving behavior.

Before this can happen, however, vehicles B and C must consider the relative location of the vehicle requesting the lane change. Merging priority is given to vehicles in the VROW lane that are closest to the bus. If vehicle C, the trailing vehicle, receives a merging request from vehicle A as well as a merging request from a vehicle upstream, vehicle C would prioritize the upstream vehicle for merging. Assuming there is only interaction between vehicles A, B, and C, vehicles B and C would cooperate to create a gap for vehicle A. After receiving information that vehicle A is attempting to merge into their lane, both B and C would look to make a right lane change. This cooperative action is defined as Cooperative Driving Algorithm 3 and performed by vehicles 2 and 7 in Figure 3.1. But before this cooperative lane change can occur, vehicles B and C must ensure that their target lane still enables their turning movement and that it also has an acceptable gap. If either of these conditions is not met, they will need to create a gap by adjusting their acceleration. There are different ways for the vehicles to adjust their acceleration, which will be discussed in section 3.2.2.

In the case where vehicles B or C cannot change lanes to create a gap for vehicle A, they also send a merging request signal to the neighboring vehicles in their target lane. The neighboring vehicles in the target lane then react by following the same algorithm process as vehicles B and C to create a gap. This creates a multi-hop signal that travels laterally across the lanes until the merging vehicle from the VROW lane, vehicle A, has completed its lane change. The signal multi-hop across multiple lanes creates a flexible algorithm that can successfully operate on roads with any number of lanes. However, the time to form a complete cooperative response from vehicles in adjacent lanes increases as the signal travels across more lanes, as each vehicle will take time to react to the merging request. By using a combination of cooperative lane-changing and acceleration, most vehicles will be able to merge before vehicles in farther adjacent lanes appropriately respond.

## **3.2. Cooperative Driving Algorithm**

By coordinating the behavior of neighboring vehicles in non-VROW lanes, it is possible to create a system that supports necessary lane changes from the VROW lane and improve the performance of the buses without much additional disturbance imposed on the private vehicles. The cooperative driving algorithm aims to do this by shifting vehicles to the right when necessary and possible. A gap acceptance parameter has been defined to determine lane-changing possibility when VROW is present. If a lane change maneuver is not possible, the vehicles switch to cooperative acceleration control to provide a merging gap. The mechanisms for determining acceptable gaps for lane-changing, as well as cooperative acceleration control, are discussed in the following subsections.

### **3.2.1. Lane-Changing and Gap Acceptance**

Vehicles performing cooperative lane changes are positioned in non-VROW lanes. However, before these vehicles can create a gap, they first need to check that a suitable gap is available

in their adjacent lane. Finding a suitable gap is based on the desired safety distance (equation 2.4) from the Wiedemann 74 model. The merging vehicle considers its own desired safety distance as well as that of its target following vehicle to determine if the gap is acceptable based on the current speed. If the target lead vehicle's distance is greater than the merging vehicle's safety distance, and the target following vehicle's safety distance parameter is also maintained, the vehicle is free to execute the merging maneuver.

In dense traffic, however, finding large enough gaps to maintain the safety distance requirement before executing a lane change maneuver can be difficult. Figure 3.4 (a) shows that in order for vehicles to merge while strictly following the desired safety distance, a doubling of the gap between the lead and lag vehicles of the target lane is required. This is difficult, as following vehicles trail their leader by their desired safety distance. Doubling this value to create an optimally safe situation before merging would take time to prepare or even prevent a lane change from occurring altogether. A system supporting VROW with lane changes should enable quick responses to merging requests. With this in mind, the safety factor reduction parameters from Vissim were also incorporated into the cooperative lane-changing algorithm.

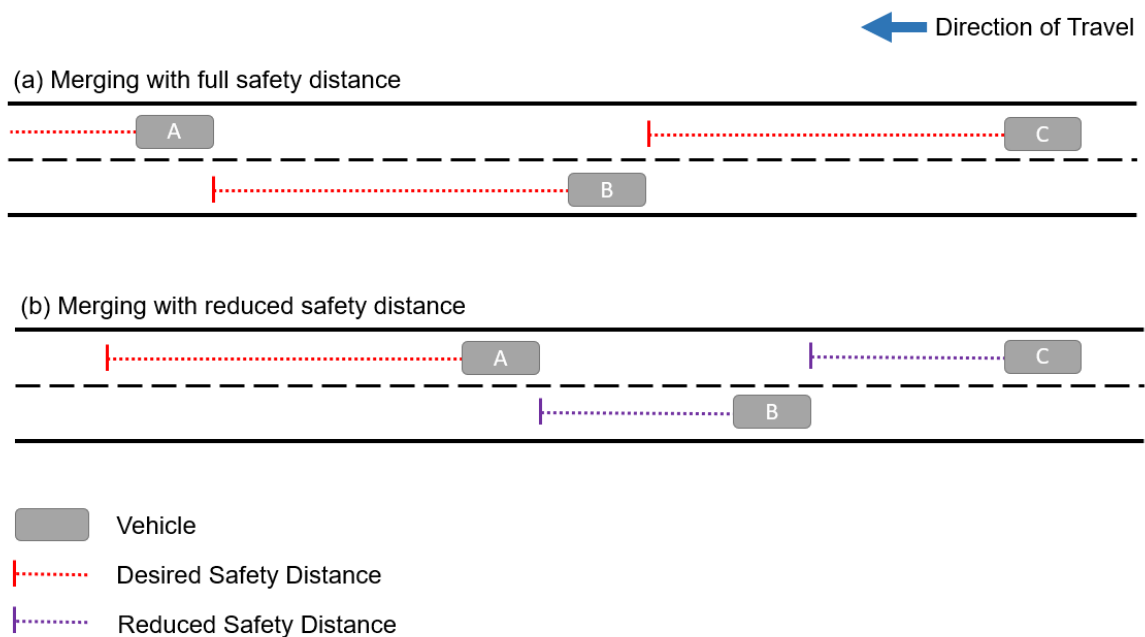


Figure 3.4. Impact of including a safety distance reduction factor for lane-changing.

As discussed in section 2.3.3, two safety factor reduction parameters can be applied to simulate heightened driver alertness when near a traffic signal controller or when changing lanes. This reduced the space required to fulfill a cooperative lane change. The default parameters of 0.6 were used for both reduction factors, meaning that the desired safety distance could be reduced by 40%. However, the two reduction factors could be combined if the vehicle was within 100 meters of a traffic controller and changing lanes, which resulted in a safety distance reduction factor that was 36% of its unreduced value. A conceptual drawing of the impact on the reduction is shown in Figure 3.4 (b). The safety distance reduction was applied to both the

merging vehicle and the target trailing vehicle. The target leading vehicle's safety distance does not influence the lane changing situation and thus was not reduced.

Some special conditions allowed merging to occur when the safety distance conditions were not fulfilled. If the lead vehicle in the target lane had a larger velocity and a more considerable acceleration, the minimum desired safety distance for the merging vehicle would be set as the standstill distance of two meters. Similarly, if the trailing target vehicle had a lower velocity and lower acceleration, the required safety distance to accept a lane change from the merging vehicle would be the standstill distance. This special case helps to drastically reduce the required space to complete a lane change.

However, in a dense traffic situation where vehicles maintain a following distance equal to the desired safety distance, it is unlikely that a sufficient gap will be available, even with the safety distance reduction factors. Some further cooperation is needed from target lane vehicles. A cooperative lane change by one or both of the target lane vehicles based on the logic presented in section 3.1 would quickly solve this issue. If the lane-change is not possible, cooperative acceleration by the vehicles in the target lane helps to create an acceptable gap.

### **3.2.2. Cooperative Acceleration**

When cooperative lane changing is not possible, the cooperative driving algorithm will coordinate the acceleration of connected vehicles to form a gap. As mentioned, vehicles will likely have difficulty merging in dense traffic, even with the safety distance reduction factors. In these situations, a merging request that is passed to the target lane vehicles would trigger cooperative algorithm 1 or 2, depending on the relative position of the requesting vehicle.

There are many similarities between the two algorithms. The only difference is the direction of the acceleration undertaken under certain conditions. However, before any cooperative acceleration can be calculated. The desired safety distance must be greater than the standstill distance of two meters. This two-meter value was chosen to define when a vehicle is the leader of a platoon in Vissim. Vehicles that approach a traffic signal without any preceding vehicles adopt a safety distance of less than 2 meters in the Wiedemann 74 model. This was used to define a threshold where platoon leaders would become pacing vehicles, only following the Wiedemann 74 model. The platoon leaders would pace the approach to the intersection to ensure that no cooperative vehicles would accelerate past the intersection during a red phase.

Provided that the safety distance is greater than two meters, a condition was also included to adjust the acceleration based on the current traffic condition. In order to determine when the conditions changed from free-flow to dense traffic, the car-following distance as a function of velocity was plotted for a stream of vehicles passing through one intersection in Vissim, shown in Figure 3.5. It can be seen that at a following distance of about 50 meters, vehicles began to reduce their speed and were thus no longer in a free-flow state.

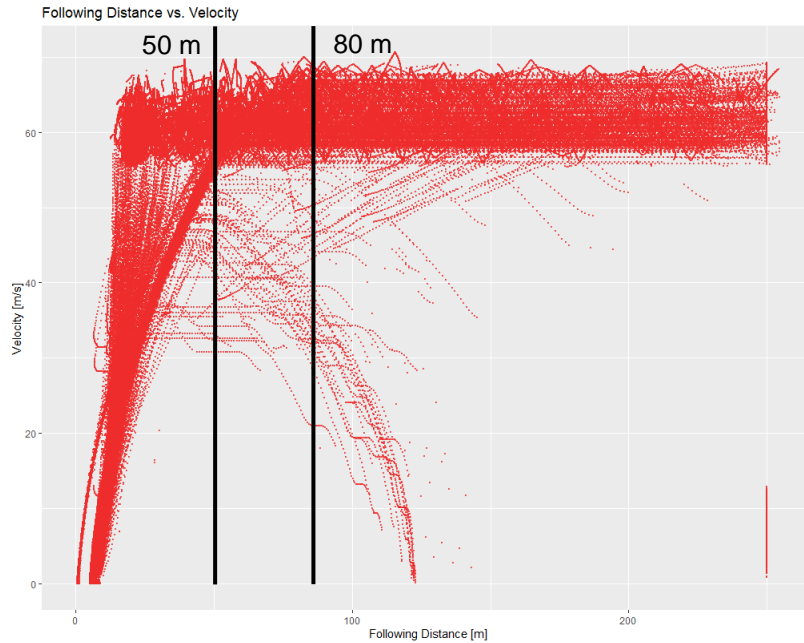


Figure 3.5. Vehicle following distance as a function of velocity in Vissim

Vehicles with a car-following distance approaching 50 meters cannot safely accelerate to create a gap behind them. If this was the case, a vehicle instead must brake to create a gap in front of it for the merging vehicle, as depicted in figure 3.6 (b). A buffer zone of 80 meters was chosen as the threshold so that vehicles do not attempt to accelerate beyond a following distance of 50 meters. However, if the following distance is greater than or equal to 80 meters, the vehicle has enough front distance to accelerate and form a larger gap behind it, as shown in figure 3.6 (a). In this diagram, vehicle C is beyond 80 meters from vehicle A, which gives enough space for it to accelerate to allow vehicle B to merge. The full logic of the cooperative acceleration behavior is provided in Figure 3.7 as an extension of Figure 3.3

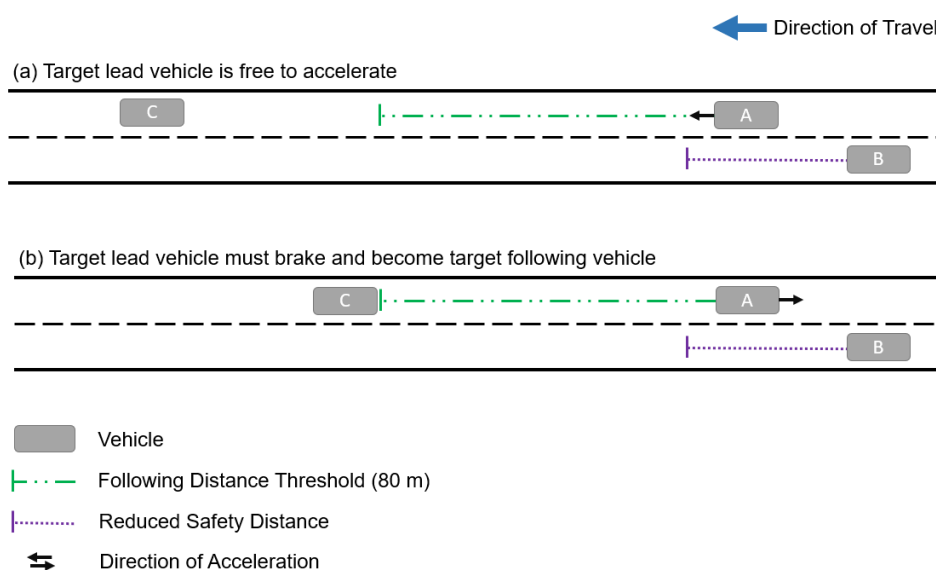


Figure 3.6. Following distance impact on the ability to create a gap

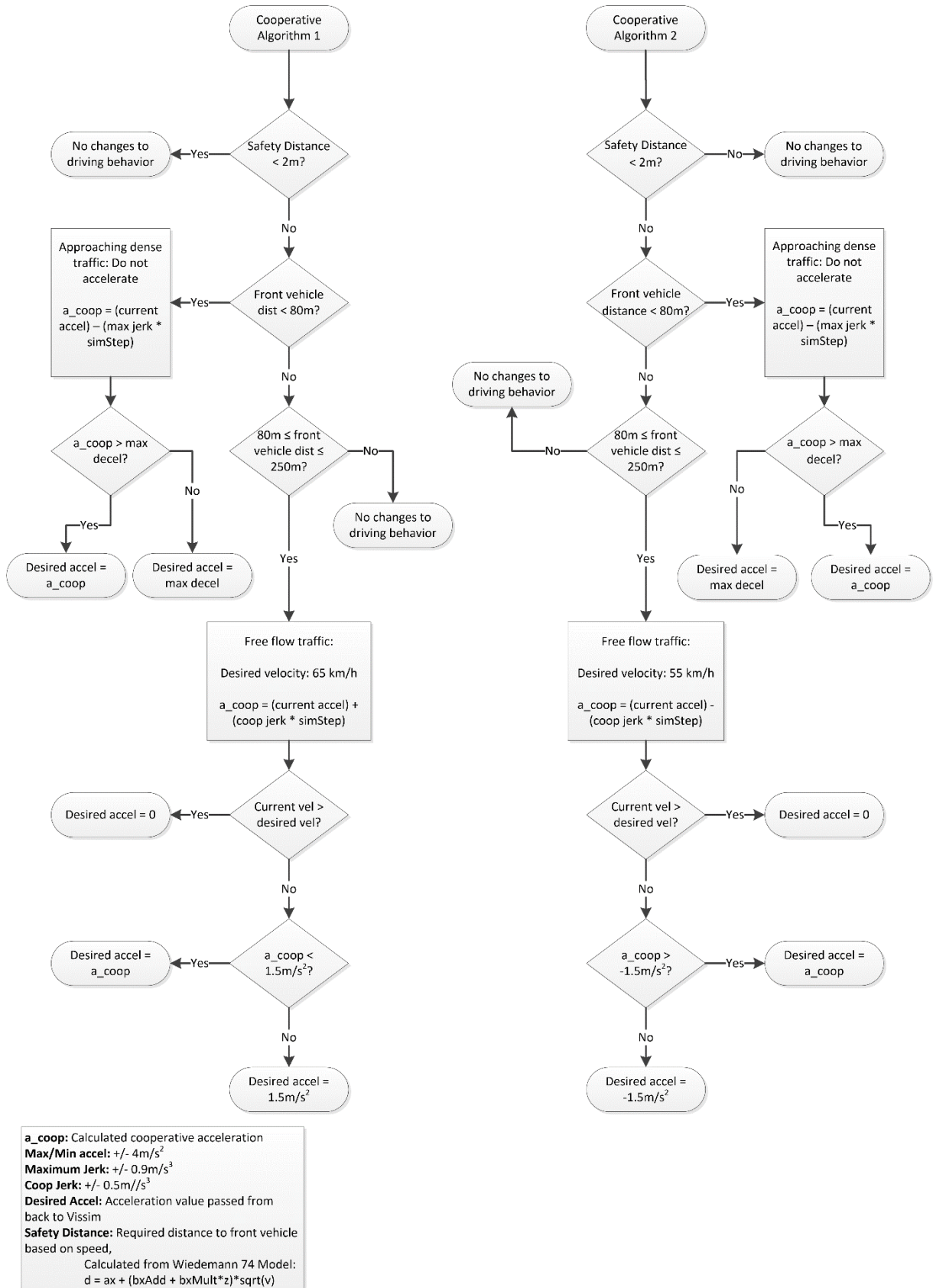


Figure 3.7. Cooperative acceleration algorithm.

### Cooperative Algorithm 1: Front Vehicle Acceleration Control

The behavior associated with cooperative driving algorithm 1 can only be undertaken if a vehicle receives a merging request from a nearby following vehicle in the left adjacent lane. Vehicle A in

Figure 3.6 represents a vehicle with these conditions, where vehicle B is the vehicle requesting to merge. If vehicle A's following distance is greater than 80 meters, the vehicle accelerates until reaching a maximum velocity. The maximum velocity for the simulation was set to 65 km/h, which was 5 km/h above the set speed limit of the modeled arterial corridor. With a following distance of over 80 meters, the increase over the speed limit would not impact the level of safety. However, roads with sharp curves may need an adjustment to this increase based on the curvature to maintain driver safety. The vehicle accelerates to a set acceleration of  $1.5 \text{ m/s}^2$  until the maximum velocity is reached. Once the rear gap is large enough for the merging vehicle, the vehicle stops accelerating and returns its velocity to the speed limit.

In the car-following state, vehicle A would instead need to brake to form a gap by braking because there is no room available to accelerate safely. This will take longer to complete since the vehicle must travel farther to create a gap in front rather than behind it. For this reason, a stronger braking force of  $-4 \text{ m/s}^2$  was set as the maximum allowed deceleration. In both cases, constant jerk is applied to prevent vehicles from accelerating too harshly. The equation governing this behavior is defined later in this section.

### Cooperative Algorithm 2: Following Vehicle Acceleration Control

Cooperative algorithm 2 is applied to control the acceleration of vehicles that receive a merging request from the leading vehicle in the left adjacent lane. In many ways, it is the complement of cooperative algorithm 1. In free-flow traffic, the algorithm reduces the acceleration to  $1.5 \text{ m/s}^2$  until the velocity reaches 55 km/h. However, in the car following state, the braking resembles that for cooperative algorithm 1 and brakes at a rate of  $-4 \text{ m/s}^2$ .

### Acceleration Function

Cooperative algorithms 1 and 2 use the same function to calculate the cooperative acceleration value to enable cooperative lane changes. The necessary acceleration to form a gap is defined as:

$$a_{coop} = \begin{cases} a_{current} + j_{coop} * t_{TimeStep}, & abs(a_{current}) < abs(a_{max}) \\ a_{max}, & otherwise \end{cases} \quad (3.1)$$

where the cooperative acceleration,  $a_{coop}$ , is a function of the vehicle's current acceleration,  $a_{current}$ , the jerk to provide smooth acceleration changes,  $j_{coop}$ , and the timestep of the simulation,  $t_{TimeStep}$ . The acceleration value that can be attained for cooperative driving is limited to  $a_{max}$ .

The jerk can be positive or negative, depending on whether the vehicle needs to accelerate or brake. For example, a vehicle with positive acceleration brakes with a constant negative jerk, resulting in the vehicle's acceleration gradually decreasing from positive to negative. The magnitude of jerk also changes depending on the situation. In dense traffic, a jerk of  $\pm 0.9 \text{ m/s}^3$  is applied, which is at the upper range of jerk values for passenger comfort. As vehicles in dense traffic need to decelerate more quickly to form a gap, particularly for vehicles executing cooperative algorithm 1 in dense traffic, a more considerable jerk value is required. Free-flowing traffic has a smaller jerk magnitude of  $\pm 0.5 \text{ m/s}^3$ . Lastly, the timestep parameter was used to ensure that the jerk value was applied correctly for each simulation step. A simulation time step of five iterations per simulation second means that each simulation iteration is 0.2 seconds. The jerk was thus multiplied by this to divide up the jerk accurately into each iteration and ensure that after 1 simulation second, the input jerk value adjusted the acceleration by either 0.5 or 0.9  $\text{m/s}^2$ .

### **3.2.3. Issues with Vehicle Platooning and Autonomous Vehicles**

In the initial concept of the cooperative driving algorithm, forming a platoon of vehicles behind a VROW bus was intended as a way to mitigate the delays caused by forced lane changes and reduced velocities from acceleration adjustments. As the bus traveled through the network, it clears its lane ahead of it and reduces its potential delays. The vehicles that needed to change lanes might experience some delay by changing into a less desirable lane. The vehicles with the most significant delay imposed by VROW would be given first priority in platooning behind the bus. As the bus's travel time and operational speed improved due to VROW, vehicles that were delayed could platoon with the bus and take advantage of the faster speeds of the bus. However, this is not possible in an urban setting. Frequent stops by the bus to service passengers guarantees a lower operating speed than the surrounding traffic. Adding in the slower acceleration of buses compared to private vehicles, it was clear that the initial concept of platooning behind buses would not be possible for the urban study area due to differences in operating speeds. Platooning vehicles behind a slower bus would only increase delays further. A highway situation with dense traffic and less frequent stops may be more suitable for platooning, but this has not been explored.

Modeling autonomous vehicles in Vissim also proved to be challenging. The initial idea was to use the IDM to simulate more realistic driving behaviors, as also done in the literature. While the IDM was implemented on the Vissim network, there were issues making IDM vehicles comply with signal controllers. The IDM is strictly a car-following model and was not designed to comply with Vissim's signal controllers. A temporary solution was devised to implement the switch between IDM control and Vissim control for platoon leaders, but issues with switching between behaviors produced undesired results, as discussed previously. As the main purpose of the research was to develop a cooperative driving algorithm, the definition of autonomous vehicles was discarded to focus on the primary task. Future research can fill this gap and work to implement AVs with the cooperative driving algorithm.

## **4. Chapter 4: Case Study**

### **4.1. Study Area Simulation Model**

The study area consisted of the arterial corridor Pioneer Road North, located in the western part of Singapore. The entirety of the road is bounded by two expressways, the Pan Island Expressway (PIE) and Ayer Rajar Expressway (AYE). Both industrial, commercial, and residential areas are accessible by the road section, supporting a variety of vehicles for a mixed traffic environment. Ten bus lines are active along this road, traveling along different sections, while an MRT station is also present nearby.

The study area was selected on the basis of the number of bus lines traversing the corridor, the absence of exclusive bus lanes, and high traffic volumes with multiple lanes in both directions. Although Pioneer Road North consists of eight intersections, the final model represents only four intersections due to the computational expense of simulating a large network. The four modeled intersections stretch from Jurong West Avenue 4 in the North to the intersection with Soon Lee Drive and Kian Teck Way in the South, with a total length of about 1200 meters. The second and third intersections from the North, Jurong West Street 63 and Boon Lay Way/Upper Jurong Road, respectively, both have different characteristics and are the reason why the model was narrowed to these four intersections. The former, Jurong West Street 63, has an MRT stop, which consequently contains many bus lines, while the latter intersection is the largest in the corridor and must handle large traffic volumes. The entire study area is shown in Figure 4.1.

The microsimulation software PTV Vissim was used to model the four intersections in Pioneer Road North (PTV Group, 2018). The base model was designed to represent the situation that is currently observed to provide a more complete understanding of the current traffic conditions such as vehicle delays, travel times, and traffic volumes against which alternative scenarios could be evaluated. Particular care was taken to ensure that the shape and scale of the network represented the actual situation. Additional turning lanes that widened the roads near the intersection were measured with GIS to make sure that available queuing lengths for these movements would be accurate. Bus bays were also modeled in agreement with appropriate bus stop specifications in Singapore (Land Transport Authority, 2019).

#### **4.1.1. Private Vehicle Modeling**

The Land Transport Authority (LTA) of Singapore provided data regarding vehicle counts from inductive loop detectors located throughout the corridor during the morning peak hour (08:30 – 09:30). This information was used as traffic volume inputs for the model. From the inductive loop detector data, turning movements at each intersection could also be determined. However, this data was incomplete, as many intersections in Singapore have unsignalized slip

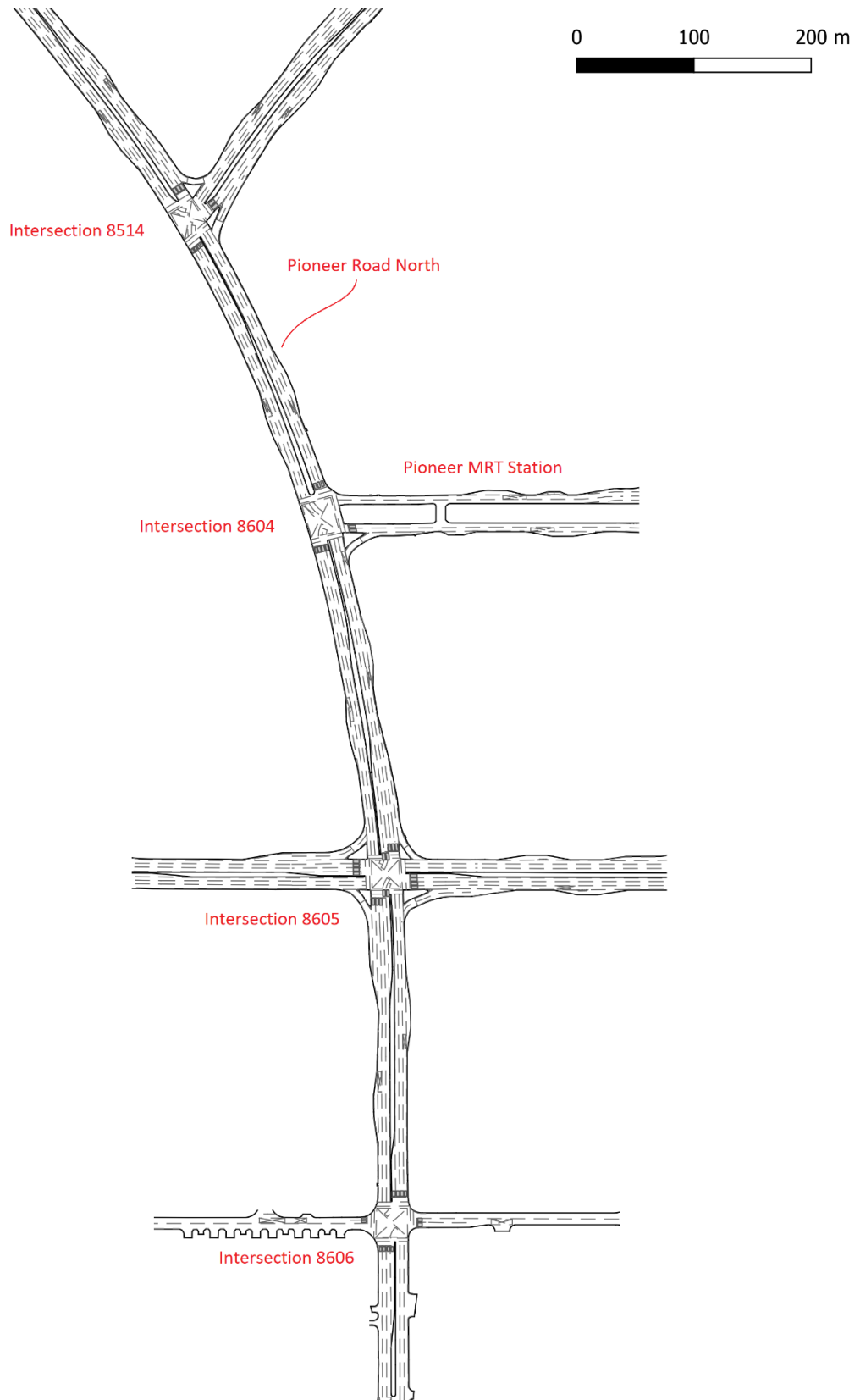


Figure 4.1. The study area of Pioneer Road North. The intersection codes were chosen by the LTA and will be used for conciseness to reference specific intersections.

roads for left-turning traffic. Vehicles turning with these slip roads only need to yield to oncoming traffic and may proceed if there are no conflicts. Figure 4.2 of Intersection 8606 shows such a situation where all four left-turn movements occur on slip roads. According to Singapore's traffic control system GLIDE (a variation of the SCATS traffic control system), detectors are placed only to adjust signal timings according to vehicle demand (Keong, 1993). Because vehicles turning left do not rely on signals, no detectors have been placed on slip roads. As a result, some assumptions were needed with regard to traffic volumes for left-turning traffic. These assumptions can have a significant impact on the accuracy of the model. The methodology for determining and calibrating these flows will be discussed in detail in the next section.

Vehicle compositions also needed to be defined for the model. As the study area consists of a mixture of industry, residential, and commercial areas, a heavy goods vehicle (HGV) share of 5% of the overall traffic was assumed. Based on a study by Lum et al., the share of motorcycles in the overall traffic ranges between 10-20% (Lum et al., 1998). A value of 10% was selected based on the assumption that larger volumes of car and HGV traffic are supplied by the two expressways. The remaining traffic composition (85%) was allocated for private cars.

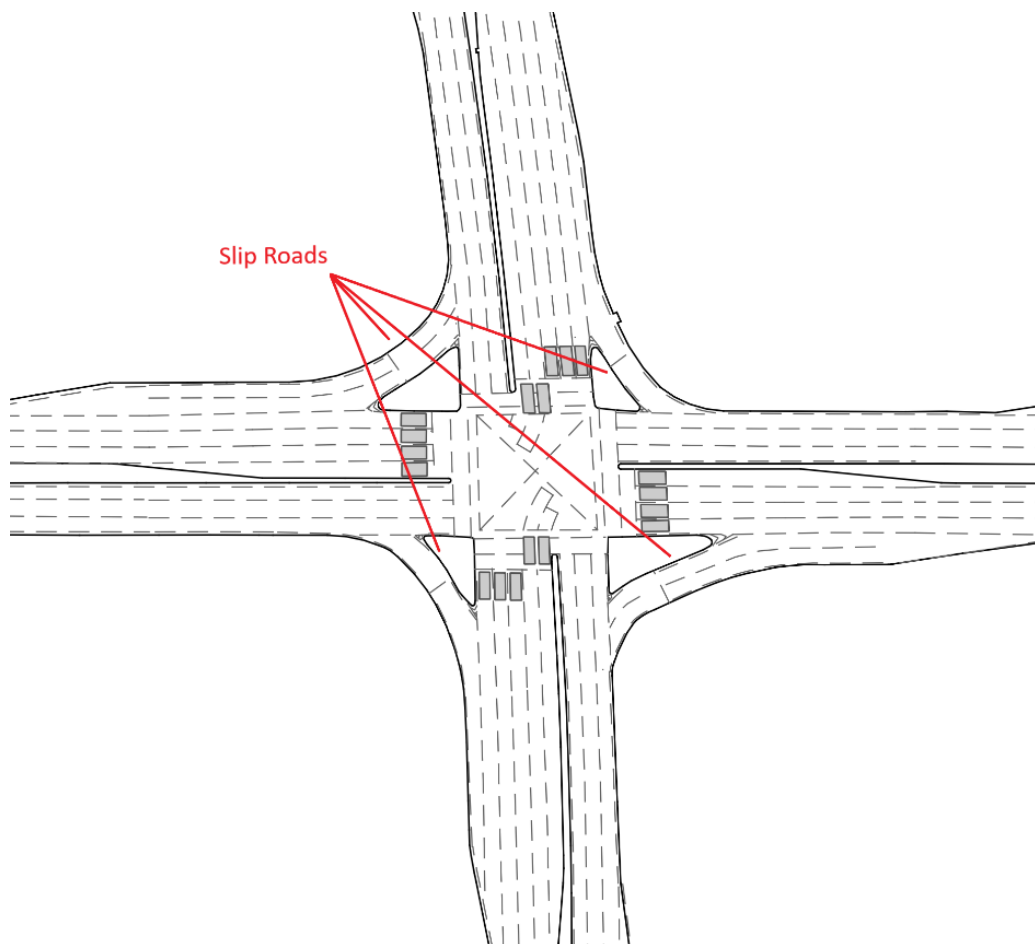


Figure 4.2. Intersection 8605 of study area showing unsignaled left turn slip roads.

#### **4.1.2. Public Transport Modelling**

Bus routes were added to the network based on each bus line's stop sequence. Bus departure time data was subsequently added. Buses were set to start entering the network after an initial warm-up time of five minutes. Initialization of the buses into the network was staggered based on the headways of each line to avoid overwhelming the model with simultaneous entries of buses from multiple lines. The departure times and bus stop sequences were obtained from Singapore's Transit Link website, which contains bus stops and headway information for all bus lines in Singapore (Transit Link Pte Ltd., 2016). On this website, headways for each bus are defined in a particular range that varies with the time of day. A constant headway was taken as the average between the minimum and maximum of this range for the corresponding time of the traffic model.

Bus stop dwelling times were added for each bus line and stop based on CEPAS smart card data from August to October 2013. The CEPAS dataset provides information about the time of the first and last passenger boarding from the timestamp of the card reader. The temporal difference between the first and last passenger boarding represents the time a bus is dwelling at the bus stop. The averages of each line for each stop in the network were calculated for the entire dataset. Only data that falls between the morning peak hour time during weekdays was used for the calculation, as this matches the traffic volume data being modeled.

#### **4.1.3. Signal Controllers**

Four signal controllers were defined along the modeled corridor. Data obtained from the LTA gave detailed information concerning signal group sequences and timings. All intersections in the study area are coordinated under the same SCATS subsystem. Because of the coordination and variable cycle times of SCATS, a simplification of fixed-time signal control was done by taking the average cycle time of each intersection. The average cycle time was then set for all intersections to maintain coordination between each signal group. Percentages of green times were kept constant between SCATS data and fixed signal control implementation. Signal offsets between linked intersections were also preserved based on the SCATS data to maintain signal coordination along the corridor. The entire Vissim network is shown in Figure 4.3.

### **4.2. Model Calibration**

Before the model can be used to evaluate alternative scenarios, it needs to be evaluated to ensure that the model can accurately reproduce what is observed in the study area. The following subsections describe this calibration procedure.

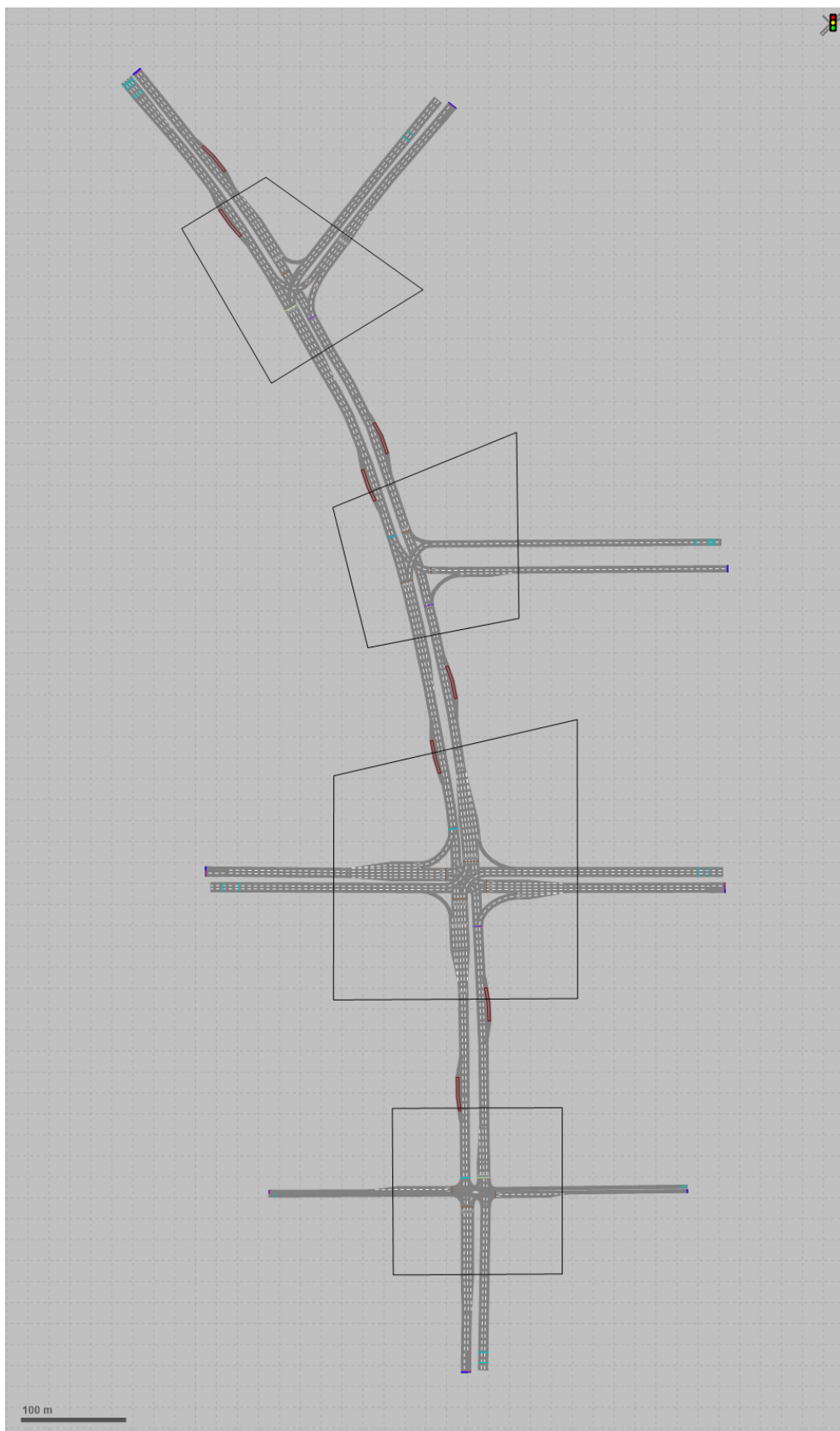


Figure 4.3. Vissim network model of Pioneer Road North study area

#### 4.2.1. Calibration Metric

Vehicle flow rate data was the most readily available data input for the model. Comparing the actual traffic count data with the modeled traffic count data would thus provide the best metric for understanding how well the model can reproduce the currently observed situation. Measurement points were placed at all approaches of each intersection. Simulated data was collected for one hour of simulation time and compared to the actual hourly traffic volumes.

#### 4.2.2. Performance Measures

The GEH statistic was used as the main performance measure for calibration. This statistic is commonly used in comparing modeled data with observed values (Balakrishna et al., 2007; Chitturi et al., 2014; Ciuffo et al., 2008; Ma et al., 2007; Paz et al., 2012; Paz et al., 2015). GEH values approaching zero represent modeled values that are increasingly more accurate to observed data. As a general guideline, GEH values less than 5.0 indicate good performance, values between 5.0 and 10.0 suggest that there are some minor issues with the model, while any values greater than 10.0 clearly signify problems with the model (Chitturi et al., 2014). A traffic model is considered to perform well when at least 85% of GEH values are below 5.0. The following equation is used to calculate GEH:

$$G_H = \sqrt{\frac{2(q-\hat{q})^2}{q+\hat{q}}} \quad (4.1)$$

Where  $G_H$  is the GEH value for hourly traffic,  $q$  is the observed traffic flow [veh/h], and  $\hat{q}$  [veh/h] is the modeled traffic flow. It is important to note that GEH can only be calculated using hourly traffic flow values.

#### 4.2.3. Calibration Approach

The GEH statistic was used to evaluate the fitness of the modeled traffic volumes, but because of the unsignalized slip roads for many left-turn movements, assumptions were made about the vehicle turning volumes making this turning movement.

The most critical of these assumptions was the traffic volume entering the network from the northern intersection from the eastern approach. An initial left-turning ratio was assumed at 10%. However, by observing the vehicle counts in the simulation at the adjacent intersection with Jurong West Street 63, it was clear that a large volume of vehicles was missing. As the unsignalized slip road did not have any detector, it was assumed that the missing volume was due to an inaccurate assumption of left-turning vehicles. The traffic volume and left turn ratio of the slip road was therefore increased to match the observed detector counts of the downstream intersection.

A similar logic was applied for the remaining intersections in the study area. By comparing the simulated and observed flows, volumes were adjusted for the unsignalized slip roads. Before

any adjustments to vehicle flows were made, however, the simulation was run 30 times with different random seeds. The average flow values at each intersection approach from these runs were used for the evaluation of any necessary changes.

#### 4.2.4. Calibration Results

The adjustment of vehicle volumes was done manually in an iterative process, only changing one vehicle input for each iteration. This was done eight times, at which point the GEH statistic showed that 95.8% of the simulated measurements matched the observed measurements with GEH values of less than 5.0. Only the volumes from one link, the western input at Intersection 8606, did not fulfill the GEH criteria. However, this flow was mainly an input for the volume at the next intersection. Because the flow for the adjacent intersection (8605) already showed accurate performance, no action was needed to improve the overall accuracy of the traffic volumes in the main corridor.

Table 4.1. Summary of calibration results for GEH statistic at each intersection approach per intersection

Intersection Approach	Iterations							
	1	2	3	4	5	6	7	8
8514_North	9.213	9.032	9.005	9.005	9.032	9.032	9.032	1.588
8514_South	1.179	1.146	1.146	1.146	1.179	1.245	0.783	0.783
8514_East	0.871	0.871	0.871	0.871	0.871	0.871	0.871	0.871
8604_North	15.603	3.824	3.849	3.849	3.849	3.875	3.849	4.485
8604_South	2.769	2.736	2.736	2.736	2.736	2.736	2.250	2.250
8604_East	2.254	2.254	2.254	2.254	2.089	1.922	1.922	1.922
8605_North	16.426	9.654	9.624	9.624	1.931	0.404	0.350	0.027
8605_South	0.645	0.706	0.706	0.706	0.706	0.706	1.284	1.284
8605_East	0.305	0.305	0.305	0.305	0.305	0.305	0.305	0.305
8605_West	0.206	0.206	0.206	0.206	0.206	0.206	0.206	0.206
8606_North	34.673	29.905	17.109	17.109	12.244	3.122	3.034	2.923
8606_South	1.042	1.042	1.042	1.042	1.042	1.042	1.042	1.042
8606_East	6.116	5.958	5.958	5.958	5.958	5.958	4.401	4.401
8606_West	13.067	13.067	13.067	13.067	13.067	13.067	13.067	13.067
% Links w/ GEH < 5.0	57.1%	64.3%	64.3%	64.3%	71.4%	78.5%	85.7%	92.9%

#### 4.3. Implementation of VROW and Cooperative Driving in Vissim

The VROW algorithm uses Vissim's External Driver Model (EDM). The EDM enables the definition of driving behavior that differs from the driving behavior models provided by Vissim. Vehicles using the EDM can thus be designed differently with a user-defined behavior under certain situations, such as in the presence of a bus or merging vehicle. The EDM is specified

by vehicle class, so every vehicle in the network in the specified classes follow the EDM behavior. In each simulation second, the EDM calculates and executes the behavior for every vehicle it controls.

With the EDM, each vehicle detected its six nearest-neighbor vehicles (front, behind, and front/behind right/left). A multi-hop architecture was used to pass the information of a detected bus to downstream vehicles. Vehicles within a 250-meter range of the detected bus change their behavior from Vissim-controlled to EDM-controlled. Instead of modeling a vehicle communication architecture to pass information between the relevant parties, the EDM was used to provide a similar outcome with a more straightforward implementation. However, this assumes a communication system without any communication losses, which can be challenging to attain in a real-world scenario. The 250-meter restriction on the reaction of vehicles to the presence of a bus was implemented to simulate a more realistic communication range.

### **4.4. Scenario Definition and Preparation**

Five scenarios were defined for the simulation of the interaction of connected and non-connected vehicles at different penetration rates with VROW. The penetration rates of connected vehicles are as follows: 0%, 25%, 50%, 75%, and 100%. Each scenario was named after the percentage of connected vehicles in the network. The 0% scenario represents the base scenario, where there are no connected vehicles in the network. In the same manner, the 100% scenario represents the case where all of the vehicles in the network are connected and comply with the VROW signal. Within scenarios with mixtures of connected and non-connected vehicles, percentages of each type of vehicle were set proportionally for each vehicle class. For example, the 25% scenario had 25% connected cars, 25% connected motorbikes, and 25% connected HGVs. The remaining 75% of the traffic composition was left for each of these vehicle classes. Public buses, traffic volumes, and turning ratios were not altered in any way for the scenarios. Each scenario only changes the proportion of vehicles reacting to the VROW signal. Each scenario was run for 20 iterations with a simulation time step of 0.2 seconds. One iteration ran for 3900 simulation seconds, including 300 seconds of warm up time.

## 5. Chapter 5: Results and Analysis

As previously discussed in Chapter 3, cooperative driving behavior has been classified into four different functions. A summary of the control functions was given in Table 3.1. The results presented in this section are outcomes of different connected vehicle penetration rates with VROW operation on the case study area of Pioneer Road North in Singapore.

### 5.1. Gap Acceptance

The Wiedemann model calculates a required safety distance for each vehicle depending on its current velocity and several other desired distance parameters, as explained by equation 2.4 in section 2.3.3. This equation was used to calculate an acceptable gap parameter for vehicles attempting to change lanes due to a VROW request. The calculated acceptable gaps from one complete simulation run with 100% driver compliance are shown in Figure 5.1.

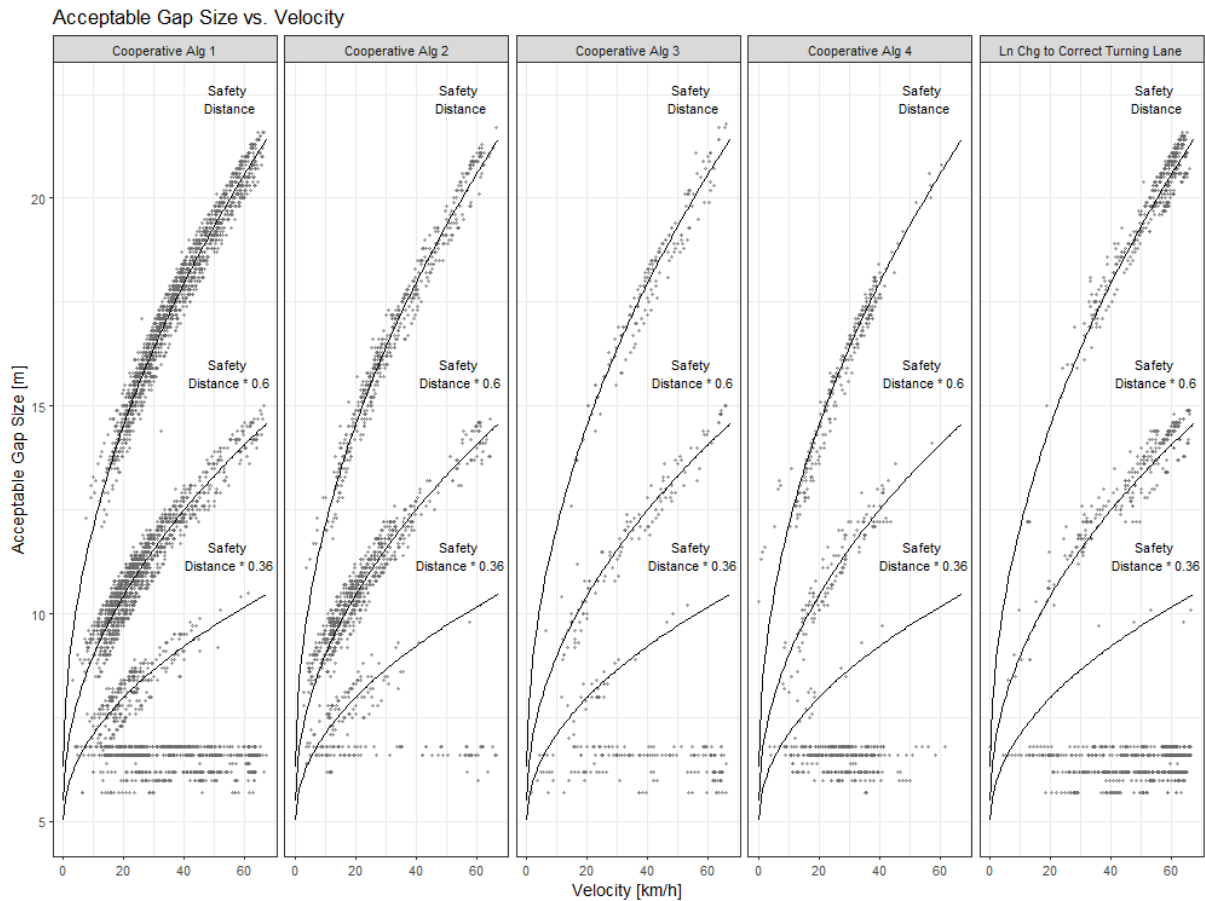


Figure 5.1. Acceptable gap related to velocity in the 100% Scenario. Different safety distance functions were used based on certain conditions. The vehicles' cooperative behaviors are also shown.

Vissim's External Driver Model calculates the distance to the preceding vehicle as a head-to-head distance. Vehicle lengths are not considered and must be added to the safety distance calculation for an accurate available merging gap. The effect of this is represented by the spread of the data rather than single points that precisely follow the safety distance equation. The horizontal lines near the bottom of the subplots of Figure 5.1 are the lengths of the preceding vehicle plus the desired standstill distance. Additionally, the minimum distance represented by these horizontal lines should only be reached at zero velocity. However, an additional condition was added for the vehicle to accept an adjacent gap with the minimum safety distance (standstill distance plus vehicle length in the adjacent lane) if the adjacent vehicle was traveling with an equal or greater relative velocity and a more considerable acceleration. This is why the minimum safety distance forms a horizontal line across each subplot.

The gap acceptance was based on percentages of the safety distance value used in Vissim. If a vehicle was within 100 meters of a signal head or changing lanes, the acceptable gap was reduced to 60% of the safety distance. If both conditions were true simultaneously, the acceptable gap was reduced to 36% of the safety distance. This was taken from the default safety distance reduction factor values in Vissim and used to plot the shorter safety distance functions in Figure 5.1. From this figure, it is clear that Cooperative Algorithms 1 and 2 dominate the cooperative behaviors to assist VROW. Cooperative Algorithm 3 is activated much less frequently in comparison. There are two reasons for this. The first is that due to the high traffic density, particularly for southbound traffic, there are few available gaps to perform cooperative lane changes. Cooperating vehicles can then only adjust their acceleration. Secondly, vehicles changing acceleration are acting for more extended periods of time than vehicles that are changing lanes.

In the rightmost subplot, we can see the instances when vehicles are allowed to disregard the cooperative driving requests to change into the correct turning lane. Once in the correct turning lane, however, the vehicle then will comply with any VROW requests, provided it is a connected vehicle. The change into the correct turning lane mainly occurs at higher velocities, indicating that this occurs before any acceleration changes or signal controller queues from downstream interfere with finding the correct turning lane. Should there be a conflict between multiple cooperative algorithm calls, the vehicle will always prioritize finding the correct turning lane before continuing with other cooperative behavior.

## **5.2. Acceleration and Jerk**

### **5.2.1. Individual Vehicle Control**

The proposed cooperative driving algorithm calculates required acceleration changes to assist with merging when lane changes are not possible. Vehicles receive a signal to adjust their acceleration based on the distances to the preceding and neighboring vehicles. Figure 5.2 shows the acceleration and jerk control of a cooperative vehicle to assist in the merging of a

neighboring vehicle. In this instance, the vehicle created a larger front gap by decelerating. The deceleration shown by the points in Figure 5.2 (a) is limited to a constant rate of  $0.9 \text{ m/s}^3$  to avoid any dangerous and sudden changes in the vehicle's trajectory. Figure 5.2 (b) shows the jerk of the same vehicle during the same simulation time. The horizontal line highlighted by the green and blue points indicates the vehicle is decelerating with a constant jerk while driving cooperatively.

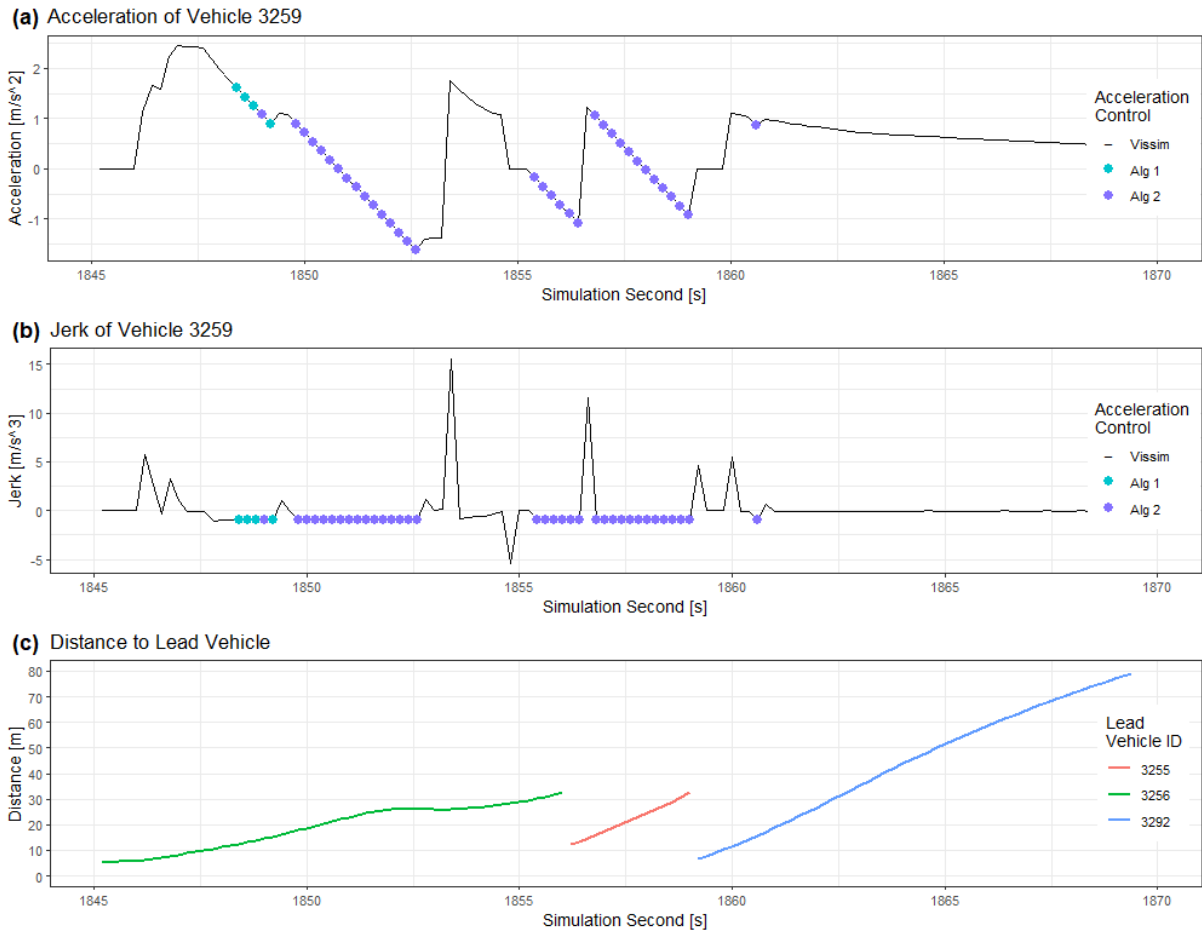


Figure 5.2. Gap creation through acceleration and vehicle control of an individual vehicle.

Through the deceleration phase, the vehicle's front gap gradually increases, as depicted in Figure 5.2 (c). During the initial cooperative deceleration, the front gap increases from 10 meters to 25 meters in four seconds, but no vehicle was able to merge and fill this gap. The second round of cooperative deceleration, occurring just after at simulation second 1855, was able to successfully support a merging vehicle, which is indicated by the sudden drop in the front gap and change in the leading vehicle's identification number. The vehicle continued to decelerate to accept another merging vehicle shortly after.

But even as the cooperative acceleration is able to successfully create acceptable merging gaps, the jerk values under Vissim's control are excessively high, reaching higher than  $10 \text{ m/s}^3$  twice within a five-second interval. Jerk higher than  $2.0$  is already considered to be extremely aggressive driving behavior. Values greater than  $10 \text{ m/s}^3$  are well beyond the comfort and safety levels for humans. The high jerk values occurred just after the driving behavior switched from cooperative acceleration control to Vissim control. This is likely the result of how Vissim's EDM operates as well as how Vissim manages jerk of the vehicles. At the moment vehicle 3255 filled the front gap at simulation second 1866, there was a sudden jump in the ego vehicle's acceleration before continuing the cooperative acceleration algorithm. The switching of the leading vehicles after a lane change may thus cause some instability in how the EDM passes on the VROW and cooperative driving signal.

Even with this issue, however, Vissim does not factor in the vehicle's acceleration in the previous time step before assigning a new acceleration. In other words, Vissim does not strictly manage jerk. Vissim's driving model assigns an acceleration based on the gap available in front of a vehicle. Under exclusive Vissim driving behavior control, this is not a significant problem, as the continuous control of a vehicle with a changing gap size leads to gradual changes in acceleration over time. But by introducing an external driving behavior under certain conditions (i.e., the cooperative acceleration model), the behavioral continuity of the vehicle's control is disrupted. In Figure 5.2, the vehicle decelerates to create a larger gap, but when the vehicle control switches back to Vissim's driving behavior control, there is a sudden increase in acceleration since that newly created gap is associated with a certain acceleration. Even as the cooperative driving algorithm proposed here was designed to limit jerk, more work needs to be done to reduce the jerk caused by switching between driving control models. Provided that this can be fixed, the performance of the model should improve as well, since the sudden increase in acceleration negates the effectiveness of slowly decreasing the acceleration over the past simulation steps.

### 5.2.2. Jerk and Acceleration Distributions

In order to evaluate the values that were output from the acceleration control algorithm, the jerk of each vehicle at each simulation second in the 0% penetration scenario was compared to that in the 100% penetration scenario. The base scenario relies entirely on Vissim's Wiedemann 74 driving behavior model. The acceleration and jerk values from this scenario thus represent a range and distribution from a well-validated model. Figure 5.3 below compares the distribution of the vehicles' jerk for the 0% and 100% penetration rate scenarios.

The base scenario has nearly all of its jerk values within  $\pm 5 \text{ m/s}^3$ . Only 1.2% of the jerk values fall beyond this range. In contrast, 5.2% of jerk values for the 100% scenario exceed  $\pm 5 \text{ m/s}^3$ . The introduction of the acceleration control algorithm on the vehicle behavior has thus led to

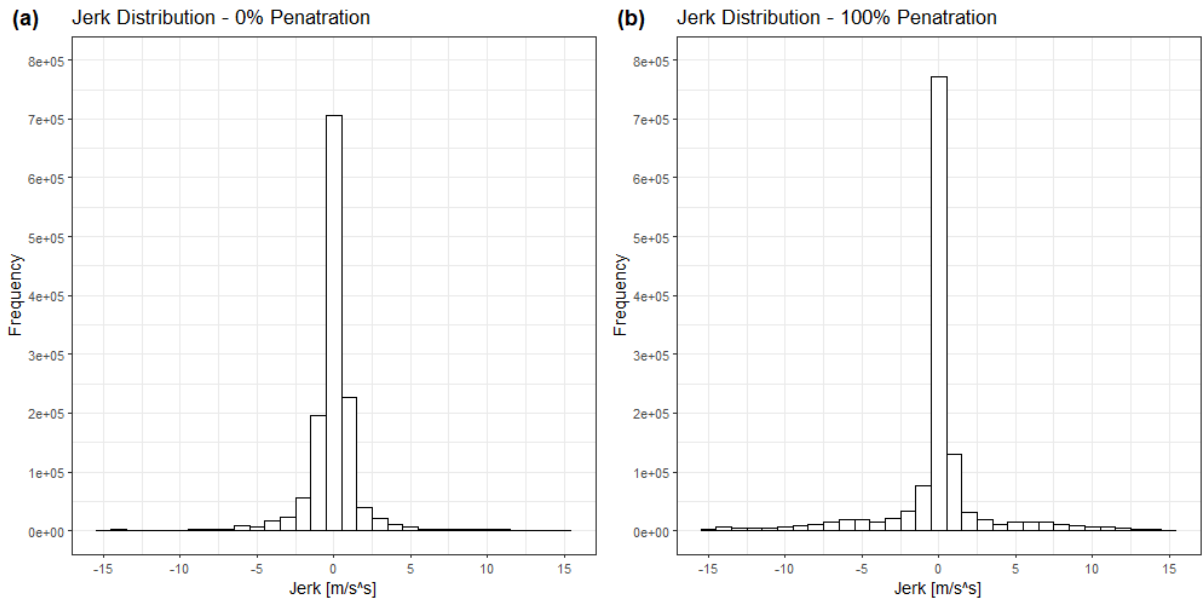


Figure 5.3. Comparison of jerk values of all vehicles in one simulation run in (a) the 0% penetration scenario and (b) the 100% penetration scenario.

slightly more unstable vehicle control as a result of the alternation between cooperative acceleration control and Wiedemann 74 acceleration control. However, acceptable jerks for private vehicles are within the range of  $\pm 0.9 \text{ m/s}^3$  for non-emergency situations. In the 0% scenario, 13.9% of jerk values exceeded this comfort threshold, while only 11.7% of jerk values did so in the 100% scenario. This further supports the possibility that Vissim's Wiedemann 74 model does not rigorously consider jerk, which has contributed to the additional 4% of jerk values beyond  $\pm 5 \text{ m/s}^3$  in the 100% scenario. The slight increase in jerk range in the 100% scenario hence does not signify any concerning changes in the system's stability.

This distribution of vehicle accelerations in the 100% penetration scenario, on the other hand, maintained a strong resemblance to the base scenario. The two acceleration distributions in Figure 5.4 are similar, but the 100% compliance scenario shows a higher occurrence of non-zero acceleration values, particularly at around  $1.5 \text{ m/s}^2$  and  $-2.8 \text{ m/s}^2$ . The positive acceleration of  $1.5 \text{ m/s}^2$  aligns well with the target acceleration set in the cooperative acceleration algorithm. Vehicles that can accelerate to create a gap target this value until a maximum speed is achieved. However, the increased occurrence of the negative acceleration is not so easily linked to the algorithm. A maximum deceleration threshold of  $-4 \text{ m/s}^2$  was set, but vehicles rarely approached this value. This can be attributed to two reasons. The first is that, with the smoothing effect from constant jerk, the rate of change in acceleration was slow enough that an acceptable gap for adjacent vehicles to change lanes was provided before reaching a maximum deceleration value. The second reason can be attributed to the unexpected switching between cooperative acceleration control and acceleration control by Vissim's internal model. The brief discontinuity in acceleration control limits the possibility for vehicles to reach their maximum cooperative deceleration, as discussed in section 5.2.1.

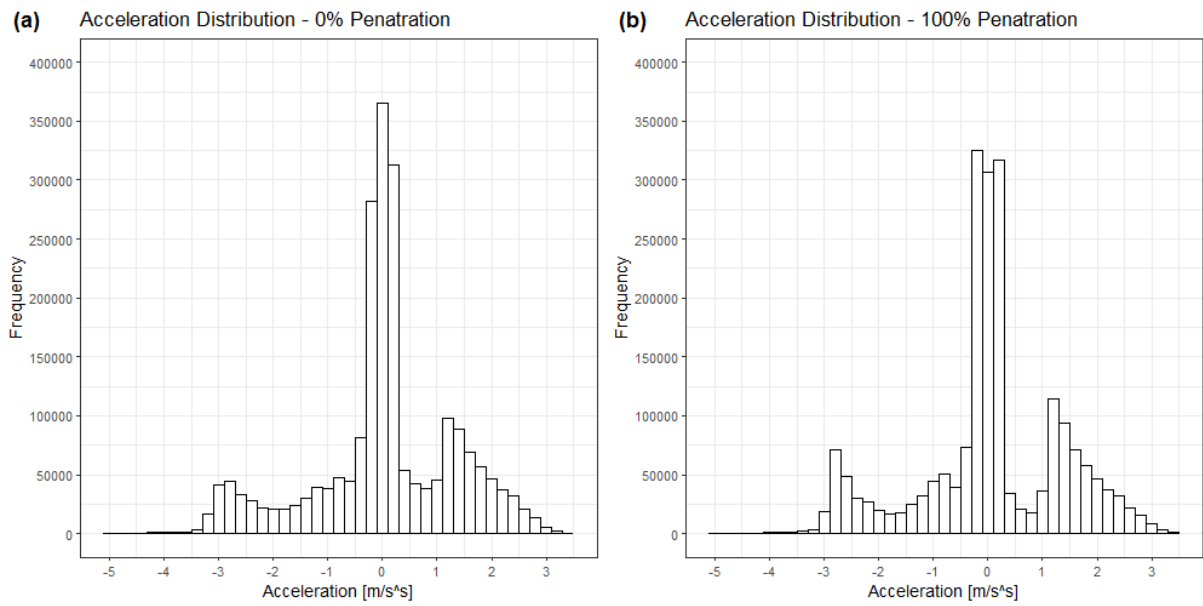


Figure 5.4. Comparison of acceleration values of all vehicles in one simulation run in (a) the 0% penetration scenario and (b) the 100% penetration scenario.

### 5.3. Vehicle Travel Times

The times for the buses and general traffic to travel across the two central intersections of the corridor were measured for northbound and southbound directions. The northbound direction has a total distance of 857.7 meters, while the southbound direction has a slightly shorter distance of 847.8 meters. Despite the shorter distance of the southbound measurement, this direction showed significantly longer travel times for both buses and general traffic compared to the northbound traffic. This is the result of the implementation of the signal controllers in each direction. Data provided by the LTA included signal timing offsets, which coordinate to form a green wave for northbound traffic through the corridor. As a result, the northbound direction has mainly free-flowing traffic with low travel times. The southbound direction, on the other hand, has no signal coordination benefits and suffers from high congestion levels and longer travel times.

However, despite the green wave for northbound traffic, not all vehicles were able to travel in this direction without stopping at a signal controller. This is due to the varying desired speed for individual vehicles as well as some delays from discharge times at the intersections. The southbound traffic, with no green wave signal optimization, faces multiple delays from signal controllers and the resulting queues and congestion. The delays caused by the signal controllers resulted in the traffic forming into separate groups depending on the number of stops experienced at each intersection for a particular vehicle. These different groups are shown in the distributions of Figure 5.5 and Figure 5.6, along with their median value.

The separation of travel times into different groups was done using the Jenks Natural Breaks Classification Method (Declercq, 1995). It works similarly to K Means Classification but can be applied to one-dimensional data. The Jenks Method reads a dataset and outputs the breakpoints for different groups within it by minimizing the variance within a group and maximizing the variance between groups. The number of breakpoints is set by the user, so the goodness of variance fit (GVF), as defined in equation 5.1, is typically used to find how well the groupings fit the data.

$$GVF = \frac{SDAM - SDCM_{all}}{SDAM} \quad (5.1)$$

In the equation above, SDAM is the sum of squared deviations for the mean of the whole dataset.  $SDCM_{all}$  is the total of the summed squared deviations for the mean of each class, or in other words, the sum of the SDCM for each class. For each scenario and direction, a GVF threshold of above 0.95 was chosen because it is a standard value used in literature (Declercq, 1995).

### 5.3.1. Northbound Travel Times

The separation of vehicles into different groups was evident for both buses and private vehicles. For the northbound direction, buses were divided into three distinct groups. Figure 5.5 (a) shows the travel times of buses traveling northbound through in all 20 simulation runs for each scenario (a total of 260 buses per scenario). The northbound buses have been divided into three different groups with a gap of about 40 seconds between each group's median travel time. Group 1 has the fastest travel time and is what a majority of the buses were classified as. These buses traveled without any delays through the corridor. Groups 2 and 3 were delayed by one or two signals, respectively, in the corridor because of their dwelling times at bus stations and due to the occasional queueing of buses at the bus stop while passengers are boarding preceding buses. Each station can accommodate two buses, but with a high bus frequency of 30 buses per hour per direction along the corridor, an additional two buses can end up waiting for the boarding area at the bus stop. All three bus groups traveling northbound show no significant improvement in corridor travel times, despite increasing penetration of cooperative vehicles. This is expected, as the delays induced on the buses are the direct result of the signal controller or bus stop dwelling times. Further, in the free flow traffic condition, general traffic can reach its desired speed of 60 km/h. This is much higher than the buses' operational speed of 45 km/h, thus not providing many opportunities for the VROW signal to request priority. However, VROW can be activated when a vehicle is expected to be delayed at a signal controller. But with many vehicles in this direction able to pass in the green wave, the benefits from VROW are minimal in this situation.

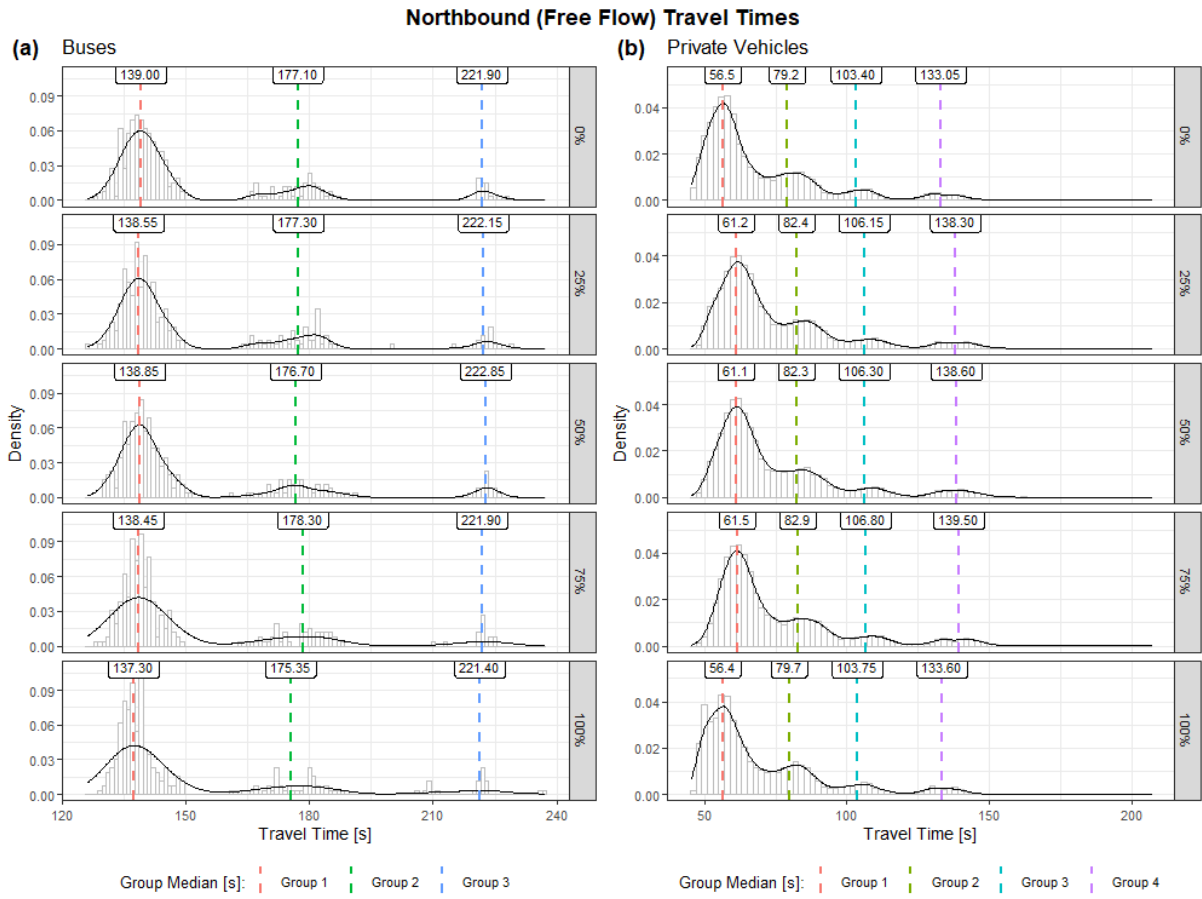


Figure 5.5. Northbound travel time distributions and median group travel times for (a) buses and (b) private vehicles at different penetration rate scenarios.

Northbound private vehicles were separated into four distinct groups, with the largest and fastest group representing the vehicles that passed through the corridor without any stops at the signal controllers. This group shows the fastest possible travel time to pass through the 857.7 meters of the corridor, which is around 56.5 seconds. Northbound buses are not able to attain this travel time due to dwelling times and lower operational speeds than private vehicles. Groups 2, 3, and 4 are the result of one or more major stop delays due to signal controllers or getting caught behind the bus queues at bus stops.

It is worth noting that even though the VROW and cooperative driving algorithms did not significantly impact bus travel times in the northbound direction, there was still minor disturbance to private vehicle travel times. In the 25%, 50%, and 75% penetration scenarios, private vehicle travel times increase slightly by 3 to 5 seconds, depending on the group. This increase, again multiplied over the length of the corridor as done for buses, may become significant for private vehicles. However, it is difficult to quantify fully because few vehicles will precisely follow the bus route and thus will not always be delayed in this way from VROW.

When cooperative vehicle penetration rates reach beyond 75%, however, private vehicle travel times return to the initial times seen in the base scenario. Further research will be needed to

determine exactly what percentage of cooperative vehicle penetration rate is needed beyond 75% to achieve this, but it is clear that a 100% vehicle cooperation rate will help to undo the disturbances caused by VROW operation.

### 5.3.2. Southbound Travel Times

Buses in the southbound direction were classified into different groups, as seen in Figure 5.6 (a). But due to the congestion levels, only two groups are formed. It is difficult to ascertain the exact reasons that caused the delays leading to the separation, but both groups must be influenced by the extremely long queue lengths at intersection 8605, which can nearly spill back into the intersection 8604 at some instances during the simulation run. Group 1, with the faster travel time, therefore may have approached intersection 8604 at a time when the queue was already discharging. Bus dwell times, as similarly mentioned for northbound buses, could also have influenced the formation of the two different southbound groups.

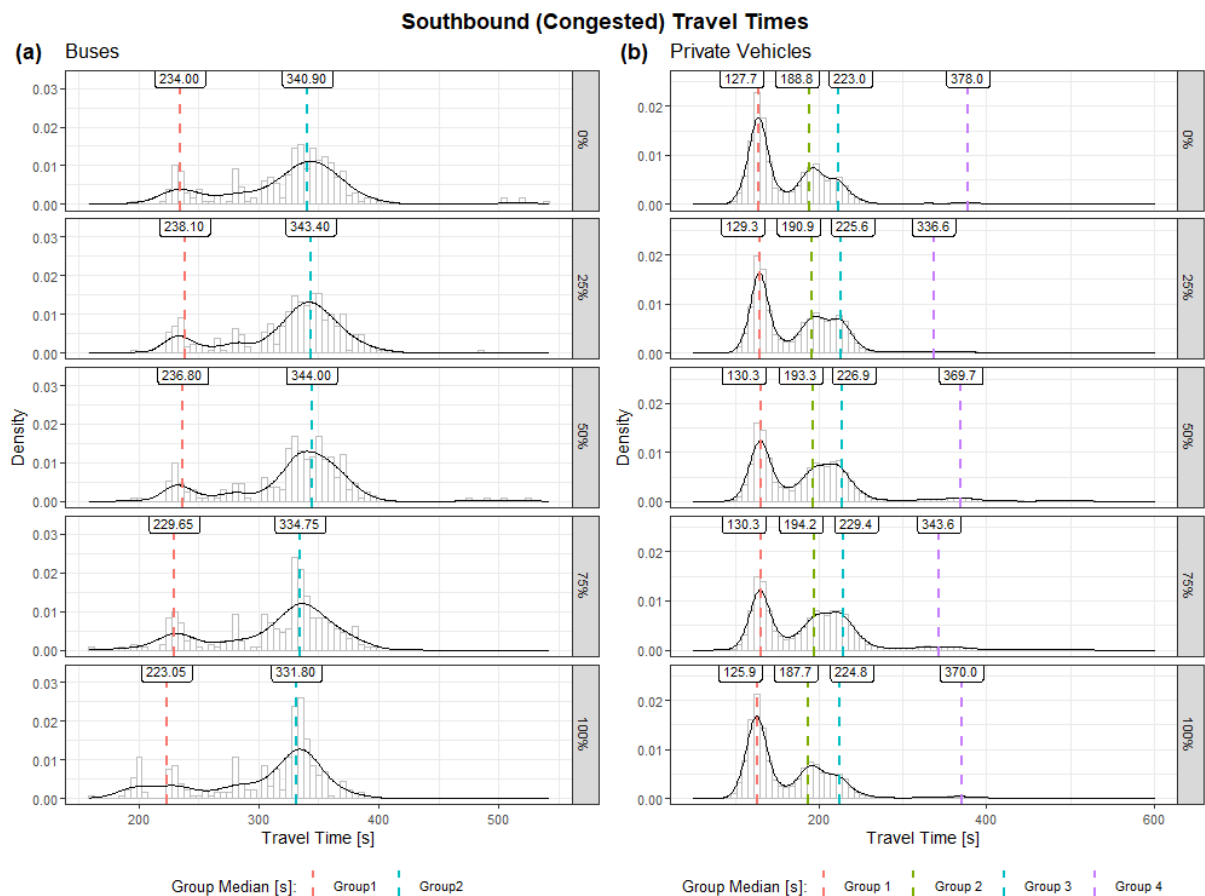


Figure 5.6. Southbound travel time distributions and median group travel times for (a) buses and (b) private vehicles at different penetration rate scenarios.

We can see that southbound bus travel times are able to show some improvements when VROW and cooperative driving are introduced. Between 0% and 50% penetration rate of cooperative vehicles, the bus shows no improved performance along the corridor. But when cooperative vehicles in the network reach 75% or greater, buses in both groups show improved travel times. Group 1 has a final travel time improvement of 11 seconds over the base scenario, with group 2 showing a similar reduction of 10 seconds. Although these improvements seem very minor considering the complex operation of VROW and cooperative driving, when accounting for the short measurement distance of less than 1 km, the travel time improvements for a bus over its entire route can be substantial.

It can also be seen that in the 100% scenario, Group 1 shows a significant shifting of buses centered around the 200-second marker. While the median travel time decreased by only 11 seconds, 28 of the 58 buses (48.3%) in Group 1 had a travel time of 207 seconds or less. In contrast, only 2 out of 47 buses (4.3%) in the same group of the base scenario had travel times that were less than 207 seconds. Additionally, 10 of 213 buses (4.7%) in Group 2 were reclassified into Group 1 from the 0% to 100% scenario, meaning that these buses experienced enough travel time improvements to push them over the threshold set by the Jenks Method.

Southbound private vehicles show a relatively similar distribution to the northbound private vehicles. Four distinct groups are again present, but travel times and distances between the groups have changed because of the congested traffic state. And due to the congested traffic state for this direction, Group 1 no longer represents vehicles that passed through the corridor without any major stop delays. Instead, this group now represents the vehicles delayed by one major stop (i.e., a signal controller or a long queue). Groups 2 and 3 are also very closely related in terms of travel time but show two distinct peaks seen most clearly in the 0% and 25% scenarios of Figure 5.6 (b). The fourth group makes up a very small part of the distribution and contains vehicles that experienced longer travel times than even most of the buses. However, with the small numbers in this group, these vehicles can be viewed as outliers of the simulation, as high vehicle volumes can sometimes cause unrealistic driving behaviors in Vis-sim when waiting to change lanes to continue on the desired path.

Similar to the northbound private vehicles, disturbances from VROW and cooperative driving are also observed in the southbound direction for the 25% through 75% scenarios. Disturbances also increased slightly on private vehicles as connected vehicle penetration rates increased. In each of these three scenarios, Group 1 was the least affected of the four groups, with only a 3-second increase in the median travel time. Groups 2 and 3 had a more significant increase of 6 and 7 seconds, respectively. Group 4 showed some significant improvement in the three scenarios, but as already mentioned, due to the small size of this group, the data is not entirely reliable. The 100% scenario again shows that with the full cooperation of drivers, the disturbance to the general traffic can be nearly eliminated despite acceleration adjustments and requested lane changes to assist VROW buses. And although the southbound buses only

formed into two groups instead of three in the northbound situation, the overall effects on the surrounding traffic were very similar.

The benefits of applying VROW and cooperative driving are most evident for the southbound traffic through the study area. As such, the potential benefits in terms of increased passenger flows along the corridor were calculated for this direction. The changes in travel times were multiplied by the number of passengers traveling south through the corridor per hour. Single-deck buses have a maximum capacity of 90 passengers (Ministry of Transport, n.d.). Running during peak hour with a mixture of single- and double-deck buses operating at or near capacity, the 90 passengers per bus was used as a basis for the calculation, but depending on how many double-deck buses run along this corridor, the actual value may be slightly higher. The general traffic was assumed to have an average of 1.7 passengers per vehicle (Fwa and Chua, 2007). The resulting impacts in travel time changes from the base scenario on overall passenger flow rates through the corridor are given in table 5.1 below.

Table 5.1. Changes in passenger flow rates at different compliance rates.

Compliance Rate	Southbound Changes in Passenger Flows [passengers/hr]		
	Buses	Private Vehicles	Net Change
25%	-55.6	-21.4	-77.0
50%	-59.2	-70.1	-129.3
75%	113.2	-56.4	56.8
100%	186.2	-3.5	182.7

The results combine the impacts on passengers in public and private vehicles for a complete picture of how many people were able to pass through the southbound corridor in one hour. With compliance rates at 50% and below, there a net drop in the flow through the corridor. However, the 75% and 100% compliance scenarios show that the improvements in bus travel times outweigh the disturbances caused by VROW and cooperative driving on the traffic. The improvements for the bus in the 75% scenario show that the equivalent of over one single-deck bus at full capacity is able to pass through the corridor, and two single-deck bus equivalents can pass for the 100% scenario. The increased capacity from VROW and cooperative driving could thus result in fewer buses required to travel along their routes. Additionally, these benefits in the 75% and 100% scenario are only from the buses operating through the corridor length of about 850 meters. A bus route with similar traffic conditions for even only several kilometers of its route would significantly increase the route's capacity while also reducing the number of buses required. A VROW and cooperative driving bus route with 5 kilometers of

similar traffic, for example, could provide the same capacity with 7 fewer buses for a 75% compliance rate and 12 fewer buses for a 100% compliance rate.

#### **5.4. Number of Lane Changes**

The average number of lane changes per scenario was calculated for all simulation runs in each direction. Increasing the number of lane changes within the same road length from VROW and cooperative lane changes can result in unsafe driving conditions should this stray too far from the baseline average (i.e., the 0% scenario). Figure 5.7 shows the average number of lane changes (NLC) per vehicle for connected and non-connected vehicles. Because of the varying penetration rates of connected vehicles, there is no data for this vehicle type's average NLC in the 0% scenario. Similarly, there is no lane changing data for non-connected vehicles in the 100% scenario.

For northbound traffic in the base scenario (Figure 5.7 (a)), the average NLC for non-connected vehicles ranges between 2 and 2.75 lane changes per vehicle, depending on the vehicle class. Non-connected HGVs have the lowest number of lane changes in this scenario, while motor-bikes have the highest. This is expected, as the large size of HGVs requires larger gaps to change lanes, but the gaps to accommodate these vehicles' lane changes are less frequent than gap sizes for other vehicle types. However, there is a significant increase in the average NLC when comparing the 0% and 25% scenarios. This sharp increase is particularly surprising when considering that non-connected vehicles should not have any particularly sharp increase in the average NLC, as they do not receive any information regarding VROW.

Furthermore, as was established in section 5.3.1, northbound buses have no noticeable benefits from VROW implementation due to the free-flow traffic, and thus disturbances caused by sending VROW signals should be low. It also is evident that the average NLC for both connected and non-connected vehicles is highest in the 25% and 50% scenarios, indicating that the introduction of connected vehicles that comply with VROW signals in free-flow conditions leads to some traffic disturbances which encourage more frequent lane changing. This disturbance is also supported by the increase of private vehicle travel times in Figure 5.5. Although performing an additional lane change may not pose significant safety concerns, the disturbances to the general traffic for insignificant bus travel time improvements under free-flow conditions is not justifiable.

Southbound traffic exhibits a similar pattern to the northbound traffic. Again we there is a large increase in the number of lane changes for non-connected vehicles between the 0% and 25% scenarios in Figure 5.7 (a), but this gradually decreases as more connected vehicles enter the network.

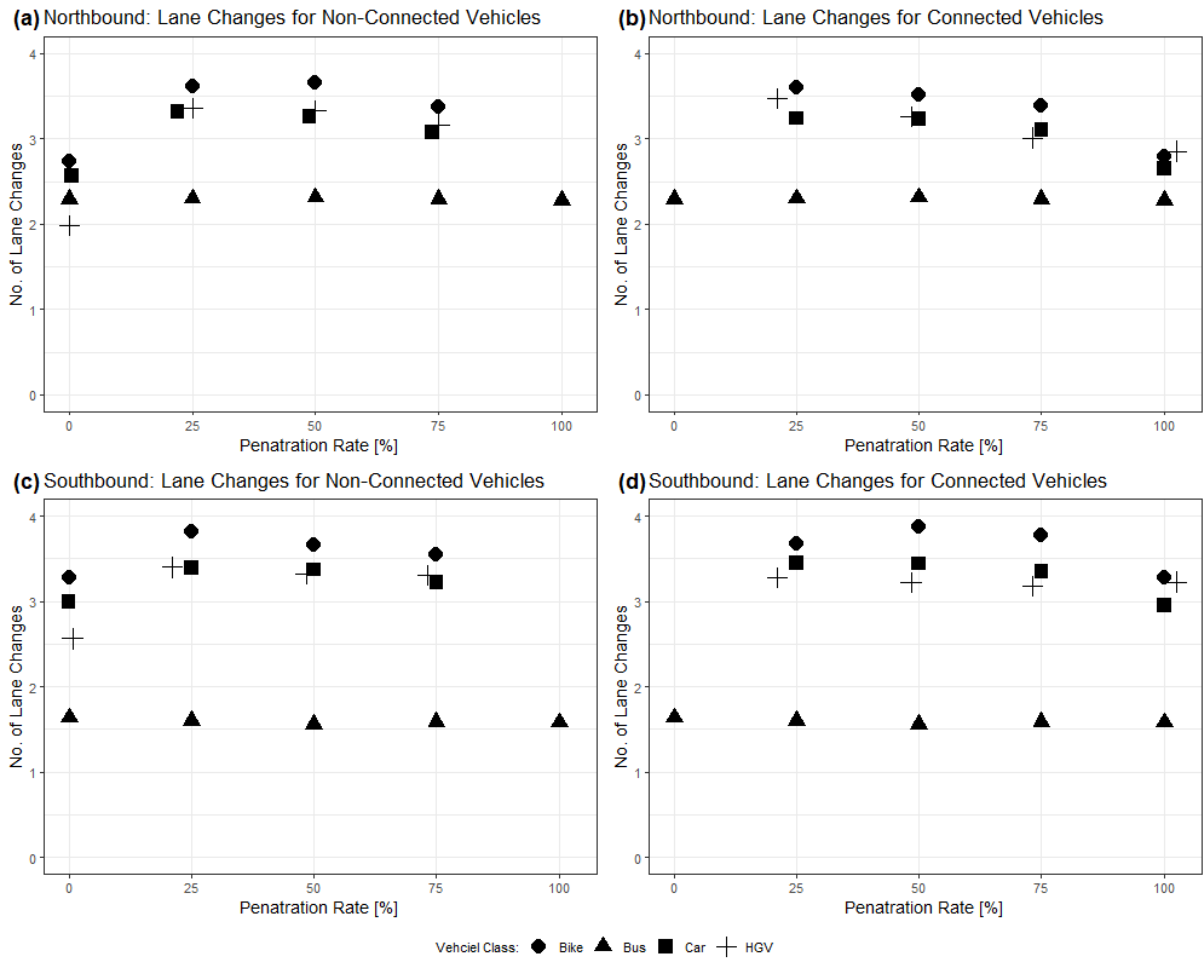


Figure 5.7. Average number of lane changes per vehicle class compared to buses for northbound (a and b) and southbound vehicles (c and d) for non-connected and connected vehicles. Please note that the points within close proximity to one another have been given a slight offset to improve clarity.

The behavior of connected vehicles, however, differs slightly from the northbound direction. The average NLC for connected motorbikes increases from 3.6 to 3.9 between the 25% and 50% scenarios. The 75% scenario also keeps this high average NLC with a value of 3.8. Other vehicle classes do not exhibit this behavior. As the VROW bus signal performs well for the southbound direction, we would expect a higher number of lane changes for all vehicle classes. The reason for this is that motorbikes have the smallest gap requirement due to their shorter length. This allows them to more easily comply with VROW signals to change lanes.

Among all the subplots in Figure 5.7, a similar trend is evident in the average NLC per scenario. Each direction and vehicle type has the sharpest increase in the number of lane changes between the 0% and 25% scenario. The remaining scenarios show a gradual decrease in the

number of lane changes with the 100% scenario closely matching the 0% scenario. This is due to the impact of connected vehicle lane changes from VROW lane change requests.

When connected vehicles respond to the VROW signal and change lanes, they impact the traffic conditions in their new lane. And because non-connected vehicles receive no information to proactively change lanes or adjust their acceleration, the addition of connected vehicles into their lane leads to a lower lane utility and may prompt reactionary lane changes from non-connected vehicles to improve their driving conditions. At 25% penetration of connected vehicles, the negative effect on non-connected traffic is the most substantial, but with a 50% road network penetration, the cooperative behavior of connected vehicles' acceleration control helps to mitigate these negative effects. Naturally, larger shares of connected vehicles on the road increasingly limit the adverse lane changes of non-connected vehicles. With fewer non-connected vehicles in the network, there are fewer vehicles that can perform these reactionary lane changes. Additionally, increasing the number of connected vehicles in the network provides more smoothing effects in acceleration control and coordinated lane changing, so the remaining non-connected vehicles have less need to change lanes to improve their driving situation.

### **5.5. Following Distance Distribution**

The following distance measures the distance from the ego vehicle to the preceding vehicle. While it is used to determine the driving behavior and acceleration of vehicles in Vissim simulations, in the case of changing vehicle behavior for cooperative driving, following distance can also be used as a safety indicator. The proposed cooperative driving algorithm changes vehicle accelerations and executes lane changes based on a safety distance. And while these modifications to the driving behavior have been designed to maintain a safe distance based on speed and vehicle following distance, it still must be tested that vehicles within the simulation are not colliding with one another while driving cooperatively. Figure 5.8 compares the distribution of the vehicle following distances throughout the corridor under one simulation run for the 0% and 100% scenarios. The 0% scenario maintains a vehicle following distance based solely on the Wiedemann 74 model, while the 100% scenario is a mixture of cooperative driving and Wiedemann 74 depending on the presence of a bus. Both scenarios have nearly identical following distances, indicating that no collisions occurred despite the modifications made to the driving behavior.

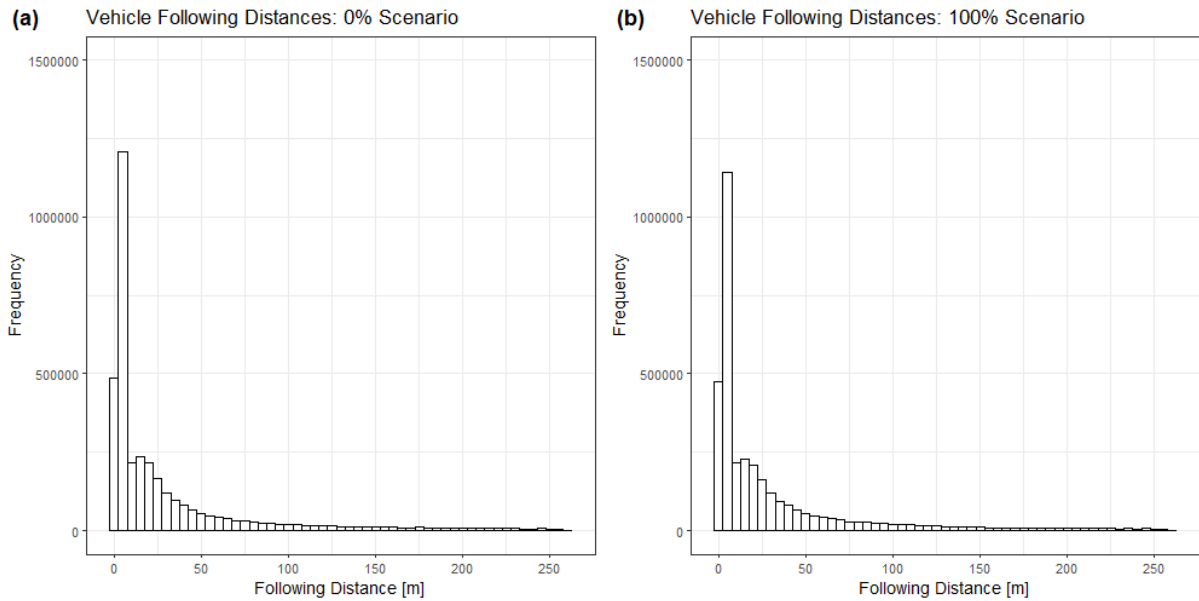


Figure 5.8. Following distance distribution for 0% and 100% scenarios.

## 5.6. VROW and the Cooperative Driving Algorithm

To fully evaluate the impact of the cooperative driving algorithm on the performance of VROW, a comparison was made within the 100% connected vehicle penetration scenario. VROW travel time performance without the cooperative driving algorithm was evaluated in this scenario and compared to the results of the 100% scenario with full cooperative driving. Results are shown similarly to those in section 5.3, where bus and private vehicle travel times are evaluated in northbound and southbound directions. The results for travel time performance with and without cooperative driving are shown with the results of the 0% scenario for reference.

As expected, the northbound direction (Figure 5.9) showed no significant difference in travel times for either buses or private vehicles. The reasons for this were discussed in section 5.3.1 as the result of unfavorable traffic conditions for VROW operation. Because the VROW algorithm combined with the cooperative driving algorithm showed little improvements in this regard, it was expected that the differences between the performance of only VROW and VROW combined with cooperative driving would be minimal. Buses showed small travel time improvements for all three groups with no cooperative driving scenario showing intermediate performance improvements from the base to the cooperative driving scenarios. Private vehicles had almost no changes in travel times among the scenarios. All groups showed changes in median travel times of 1.1 seconds or less.

The cooperative driving algorithm in the southbound direction exhibited notable improvements over the standalone performance of VROW. Figure 5.10 (a) shows that VROW was able to

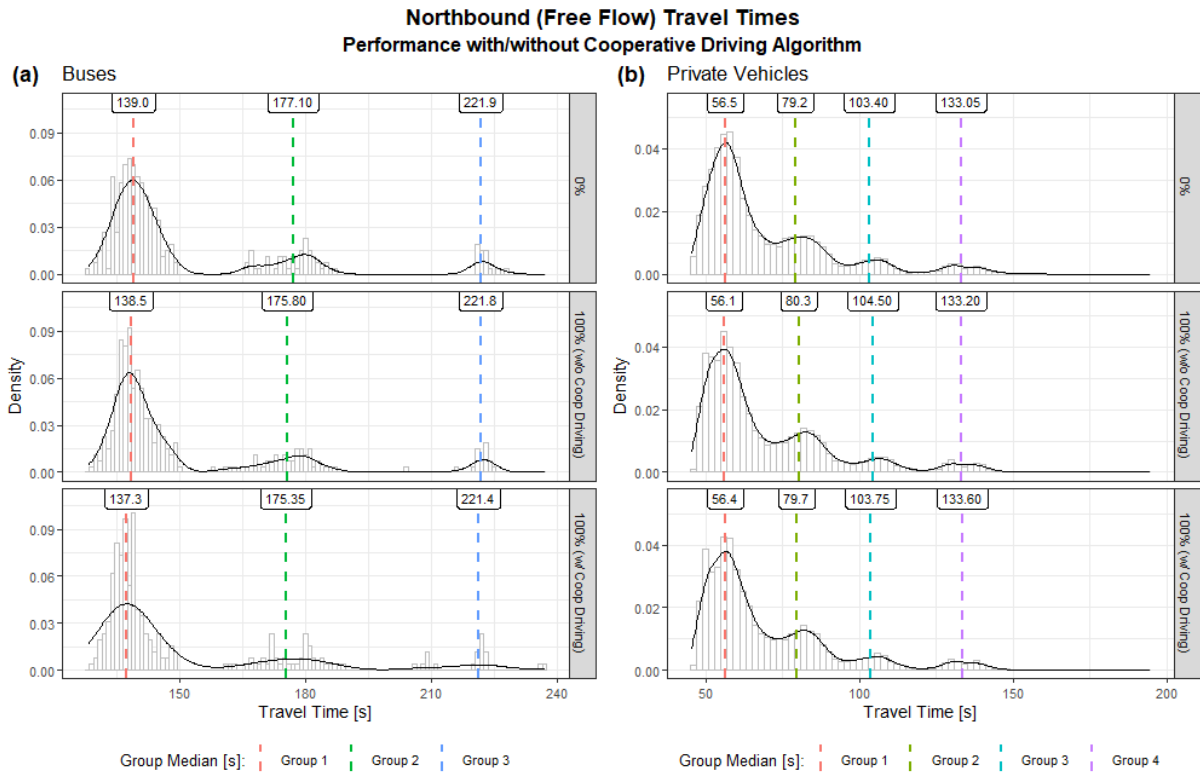


Figure 5.9. Comparison of bus (a) and private vehicle (b) performance for northbound traffic for the 0% scenario, 100% scenario without cooperative driving, and 100% scenario with cooperative driving.

improve the bus travel times by about 7 and 8 seconds for Groups 1 and 2, respectively, over the base scenario while imposing no significant travel delays on private vehicles. Adding in the cooperative driving algorithm to support VROW enabled bus travel times to further increase by 4 seconds for Group 1. Of this group, 28 buses (4.8%) had travel times below 207 seconds. By comparison, only 17 buses (3.0%) in Group 1 for the standalone VROW situation were able to attain travel times below 207 seconds. And despite the cooperative lane and acceleration changes, the cooperative driving algorithm with VROW did not introduce any additional delays for private vehicles. Bus Group 2, however, showed a travel time improvement of only 1 second despite the added benefit of cooperative driving. This group experienced more delays than Group 1 and had a higher traffic density as a result. The cooperative algorithm thus struggled to perform well in the denser traffic state, as gaps available for cooperative lane changes become less frequent. Additionally, the time required to create a suitable gap for vehicle lane changes with acceleration adjustments also increased because the vehicles in denser traffic traveled with shorter distances and lower speeds. Most private vehicle groups experienced very minor changes in travel times across each scenario. Only Group 4 in the scenario with cooperative driving showed a significant improvement. But as mentioned previously, the number of vehicles in this distribution is very low in comparison to the other three groups and may not provide statistically reliable data.

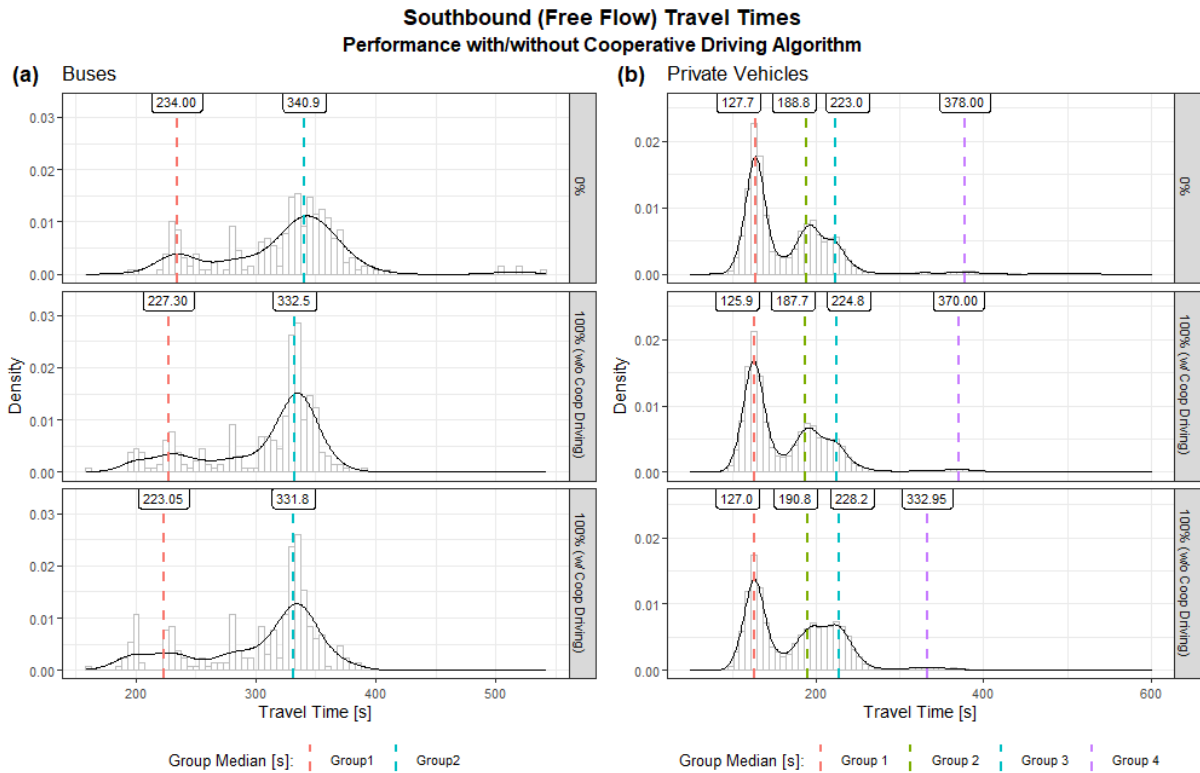


Figure 5.10. Comparison of bus (a) and private vehicle (b) performance for southbound traffic for the 0% scenario, 100% scenario without cooperative driving, and 100% scenario with cooperative driving.

A comparison between the total passenger flow rates on the southbound direction of the corridor was performed to compare the added benefit of cooperative driving against only VROW. The calculations are the same as discussed in section 5.3.2. Using the 0% scenario as the comparison scenario, VROW without cooperative driving showed a passenger flow rate increase of 156.5 passengers/hr in buses along the 850-meter length of the corridor. Surprisingly, passenger flows in private vehicles also increased slightly by 20.6 passengers/hr. This was unexpected, as the forced lane changes and lack of cooperation were expected to disrupt the general traffic. This may have been the result of the implementation of VROW without cooperative driving. In testing the VROW only scenario, the modifications made to gap acceptance for lane changes based on the desired safety distance were kept. Only the cooperative behavior of creating gaps was removed. This may have had a smoothing effect on traffic by imposing more conservative lane changing characteristics than in Vissim's driving behavior or in the original VROW algorithm.

By adding in cooperative driving, the passenger flow rate on buses was able to increase to 186.2 passengers/h, a 29.7 passenger/h increase over the only VROW scenario. However, there were more negative impacts on the general traffic as a result of the cooperative driving, making the passenger flow rates fall just below that of the 0% compliance scenario. This was to be expected, as cooperative driving, and cooperative acceleration in particular, led to more disturbances in the traffic. Although these disturbances were managed in a cooperative way,

the algorithm acted upon vehicles in more lanes than VROW. In dense conditions with vehicles in multiple lanes reducing acceleration to form a gap, travel time will inevitably increase. The added disturbance to private vehicles leads to a minimal overall increase of 5.6 passengers/h when comparing VROW with and without cooperative driving.

Table 5.2. Changes in passenger flow rates with and without cooperative driving at a 100% compliance rate

Compliance Rate	Southbound Changes in Passenger Flows [passengers/hr]		
	Buses	Private Vehicles	Net Change
100% (without Cooperative Driving)	156.5	20.6	177.1
100% (with Cooperative Driving)	186.2	-3.5	182.7

This added capacity of buses benefiting from cooperative driving only represents only a third of the capacity of a single-deck bus. But assuming a bus route will pass through 5 kilometers of similar traffic conditions during the peak hour, the added benefit from cooperative driving extends to an additional 175.2 passengers per hour on buses, which is equivalent to the capacity of 1.9 single-deck buses in Singapore. The overall throughput, when comparing the differences of VROW with and without cooperative driving, shows a minor improvement for the same 5-kilometer distance of only 33.0 passengers/h. Despite this, however, the cooperative driving algorithm is able to further improve the performance of VROW operation under dense traffic conditions without imposing considerable delays on private vehicles.

## 6. Chapter 6: Conclusions

Virtual Right of Way offers the ability to improve the operational performance of public transport buses while mitigating the negative effects of lane and capacity reductions for the general traffic. However, the availability of gaps in lanes adjacent to the VROW lane is critical in enabling this technology to operate successfully. In dense urban traffic, which is often seen during peak hours, this can be a significant problem. Human driving behavior is also an essential aspect of the ability of VROW to function as intended. Drivers who receive a VROW lane change request may be unwilling to comply, as it negatively impacts their driving situation. Even if drivers are willing to comply, they may find that the available gaps are unsafe to perform a merging maneuver. The cooperative driving algorithm proposed in this report was designed to incorporate with VROW to mitigate issues with gap availability through a combination of cooperative lane changes and cooperative acceleration control.

VROW and the cooperative driving algorithm were applied to an arterial corridor in Singapore, where the northbound traffic was in a mostly free-flow state, and the southbound traffic was in a dense state. VROW failed to make any significant travel time improvements in the northbound free-flow state due to the slower speed of the buses compared to private vehicles. The slower bus speeds meant that the very few VROW lane change requests were sent to private vehicles. And as cooperative driving is only activated with VROW, the addition of cooperative driving to VROW also showed no improvements for free-flow traffic. The dense southbound traffic, on the other hand, had significant improvements in travel time when connected vehicle penetration rates were at 75% and above. Minor improvements may occur between 50% and 75% penetration rates, but further simulation within this range is needed. In the best-case scenario of 100% penetration, VROW plus cooperative driving were able to improve the bus line capacity by 186.2 passengers/h over the base scenario. Extending these improvements to a route with 5 kilometers under similar traffic conditions would increase capacity enough to save 12 single-deck buses in Singapore. Comparing the cooperative algorithm's performance to the performance of only VROW also showed some improvements. A similar 5-kilometer route using VROW and cooperative driving would increase capacity by almost 2 full single deck buses.

This research has shown that the proposed cooperative driving algorithm is capable of improving the performance and reliability of VROW bus operations. It also requires no additional infrastructure than needed for VROW, as it only uses V2V communication. While some issues remain unresolved regarding how the driving behavior can be switched smoothly during simulation, the results still show an ability for the cooperative algorithm to perform well under dense traffic conditions. Further improvements made to improve the handoff between Vissim control and algorithm control are expected to only further improve its performance.

## List of References

- Ahmed, K.I., Ben-Akiva, M.E., Koutsopoulos, H.N. and Mishalani, R.G. (1996) Models of Free-way Lane Changing and Gap Acceptance Behavior. *Transportation And Traffic Theory. Proceedings Of The 13th International Symposium On Transportation And Traffic Theory, Lyon, France, 24-26 July 1996.*
- Atagoziyev, M., Schmidt, K.W. and Schmidt, E.G. (2016) Lane Change Scheduling for Autonomous Vehicles. *IFAC-PapersOnLine*, 49, 61–66.
- Athans, M. (1969) A unified approach to the vehicle-merging problem. *Transportation Research*, 3, 123–133.
- Bae, I., Moon, J. and Seo, J. (2019) Toward a Comfortable Driving Experience for a Self-Driving Shuttle Bus. *Electronics*, 8, 943.
- Bagloee, S.A., Tavana, M., Asadi, M. and Oliver, T. (2016) Autonomous vehicles: challenges, opportunities, and future implications for transportation policies. *Journal of Modern Transportation*, 24, 284–303.
- Balakrishna, R., Antoniou, C., Ben-Akiva, M., Koutsopoulos, H.N. and Wen, Y. (2007) Calibration of Microscopic Traffic Simulation Models. *Transportation Research Record: Journal of the Transportation Research Board*, 1999, 198–207.
- Bando, M., Hasebe, K., Nakayama, A., Shibata, A. and Sugiyama, Y. (1995) Dynamical model of traffic congestion and numerical simulation. *Physical review. E, Statistical physics, plasmas, fluids, and related interdisciplinary topics*, 51, 1035–1042.
- Bi, Y., Shen, X. and Zhao, H. (2014) Explicit rate based transmission control scheme in vehicle-to-infrastructure communication networks. *China Communications*, 11, 46–59.
- Chitturi, M.V., Shaw, J.W., Campbell, J.R. and Noyce, D.A. (2014) Validation of Origin–Destination Data from Bluetooth Reidentification and Aerial Observation. *Transportation Research Record: Journal of the Transportation Research Board*, 2430, 116–123.
- Ciuffo, B., Punzo, V. and Torrieri, V. (2008) Comparison of Simulation-Based and Model-Based Calibrations of Traffic-Flow Microsimulation Models. *Transportation Research Record: Journal of the Transportation Research Board*, 2088, 36–44.
- da Costa, J.D., de Souza A. M., Rosário, D., Cerqueira, E. and Villas, L.A. (2019) Efficient data dissemination protocol based on complex networks' metrics for urban vehicular networks. *Journal of Internet Services and Applications*, 10, 1–13.

- Declercq, F. (1995) Choropleth Map Accuracy and the Number of Class Intervals, *Proceedings of the 16th International Cartographic Conference*, pp. 918–922. Barcelona: Institut Cartogràfic de Catalunya.
- Eichler, M. and Daganzo, C.F. (2006) Bus lanes with intermittent priority: Strategy formulae and an evaluation. *Transportation Research Part B Methodological*, 40, 731–744.
- Elbanhawi, M., Simic, M. and Jazar, R. (2015) In the Passenger Seat: Investigating Ride Comfort Measures in Autonomous Cars. *IEEE Intelligent Transportation Systems Magazine*, 7, 4–17.
- Feukeu, E.A. and Zuva, T. (2020) Dynamic Broadcast Storm Mitigation Approach for VANETs. *Future Generation Computer Systems*, 107, 1097–1104.
- Fwa, T.F. and Chua, G.K. (2007) Passenger Car Travel Characteristics in Singapore. *IATSS Research*, 31, 48–55.
- Gazis, D.C., Herman, R. and Potts, R.B. (1959) Car-Following Theory of Steady-State Traffic Flow. *Operations Research*, 7, 499–505.
- Gipps, P.G. (1981) A behavioural car-following model for computer simulation. *Transportation Research Part B: Methodological*, 15, 105–111.
- Gipps, P.G. (1986) A model for the structure of lane-changing decisions. *Transportation Research Part B: Methodological*, 20, 403–414.
- Helbing, D. and Tilch, B. (1998) Generalized force model of traffic dynamics. *Physical review. E, Statistical physics, plasmas, fluids, and related interdisciplinary topics*, 58, 133–138.
- Hunt, J.G. and Lyons, G.D. (1994) Modelling dual carriageway lane changing using neural networks. *Transportation Research Part C: Emerging Technologies*, 2, 231–245.
- Jia, D. and Ngoduy, D. (2016a) Enhanced cooperative car-following traffic model with the combination of V2V and V2I communication. *Transportation Research Part B: Methodological*, 90, 172–191.
- Jia, D. and Ngoduy, D. (2016b) Platoon based cooperative driving model with consideration of realistic inter-vehicle communication. *Transportation Research Part C: Emerging Technologies*, 68, 245–264.
- Keong, C.K. (1993) The GLIDE system—Singapore's urban traffic control system. *Transport Reviews*, 13, 295–305.
- Kesting, A., Treiber, M. and Helbing, D. (2007) General Lane-Changing Model MOBIL for Car-Following Models. *Transportation Research Record: Journal of the Transportation Research Board*, 1999, 86–94.

- Land Transport Authority (2019). *Chapter 11 - Bus Stops*, Land Transport Authority.  
[https://www.lta.gov.sg/content/dam/ltaweb/corp/Industry/files/SDRE\(2014\)/SDRE14-11BUS1-5-MAY2019.pdf](https://www.lta.gov.sg/content/dam/ltaweb/corp/Industry/files/SDRE(2014)/SDRE14-11BUS1-5-MAY2019.pdf). Accessed 09.12.2019.
- Land Transport Authority (2020a) Getting Around: Driving in Singapore.  
[https://www.lta.gov.sg/content/ltagov/en/getting\\_around.html#driving\\_in\\_singapore](https://www.lta.gov.sg/content/ltagov/en/getting_around.html#driving_in_singapore).
- Land Transport Authority (2020b) Land Transport Data Mall. <https://www.mytransport.sg/content/mytransport/home/dataMall.html>. Accessed 22.05.2020.
- Levine, W. and Athans, M. (1966) On the optimal error regulation of a string of moving vehicles. *IEEE Transactions on Automatic Control*, 11, 355–361.
- Lum, K., Fan, H., Lam, S. and Olszewski, P. (1998) Speed-Flow Modeling of Arterial Roads in Singapore. *Journal of Transportation Engineering*, 124, 213–222.
- Ma, J., Dong, H. and Zhang, H. (2007) Calibration of Microsimulation with Heuristic Optimization Methods. *Transportation Research Record: Journal of the Transportation Research Board*, 1999, 208–217.
- Ministry of Transport (n.d.) Enhancing Public Transport. <https://www.mot.gov.sg/About-MOT/Land-Transport/Sustainable-Transport/Enhancing-Public-Transport/>. Accessed 30.05.2020.
- Ministry of Transport (2011) COE and ERP: Can we have just one?  
<https://www.mot.gov.sg/transport-matters/motoring/Detail/coe-erp-can-we-have-just-one/>. Accessed 22.05.2020.
- Ministry of Transport (2013) Making Public Transport The Choice Mode.  
<https://www.mot.gov.sg/about-mot/land-transport/public-transport>. Accessed 22.05.2020.
- Moon, S. and Yi, K. (2008) Human driving data-based design of a vehicle adaptive cruise control algorithm. *Vehicle System Dynamics*, 46, 661–690.
- Mosebach, A., Röchner, S. and Lunze, J. (2016) Merging control of cooperative vehicles. *IFAC-PapersOnLine*, 49, 168–174.
- Nguyen, C., Farhi, N., Haj-Salem, H. and Lebacque, J. (2017) A vehicle-to-infrastructure communication based algorithm for urban traffic control, *2017 5th IEEE International Conference on Models and Technologies for Intelligent Transportation Systems (MT-ITS)*, pp. 651–656. [S.I.]: IEEE.
- Ntousakis, I.A., Nikolos, I.K. and Papageorgiou, M. (2016) Optimal vehicle trajectory planning in the context of cooperative merging on highways. *Transportation Research Part C: Emerging Technologies*, 71, 464–488.
- Olstam, J. and Tapani, A. (2004). *Comparison of Car-Following Models*.

- Panichpapiboon, S. and Pattara-atikom, W. (2012) A Review of Information Dissemination Protocols for Vehicular Ad Hoc Networks. *IEEE Communications Surveys & Tutorials*, 14, 784–798.
- Paolo B., Mauro D. and Andrea S. (2014) On the human control of vehicles: an experimental study of acceleration. *European Transport Research Review*, 6, 157–170.
- Papadimitratos, P., Buttyan, L., Holczer, T., Schoch, E., Freudiger, J., Raya, M., Ma, Z., Kargl, F., Kung, A. and Hubaux, J. (2008) Secure vehicular communication systems: design and architecture. *IEEE Communications Magazine*, 46, 100–109.
- Park, B. and Qi, H. (2005) Development and Evaluation of a Procedure for the Calibration of Simulation Models. *Transportation Research Record: Journal of the Transportation Research Board*, 1934, 208–217.
- Paz, A., Molano, V. and Gaviria, C. (2012) Calibration of CORSIM models considering all model parameters simultaneously. *undefined*.
- Paz, A., Molano, V., Martinez, E., Gaviria, C. and Arteaga, C. (2015) Calibration of traffic flow models using a memetic algorithm. *Transportation Research Part C: Emerging Technologies*, 55, 432–443.
- Ploeg, J., Semsar-Kazerooni, E., Morales, A.I., Jongh, J.F. de, van de Sluis, J., Voronov, A., Englund, C., Bril, R.J., Salunkhe, H., Arrue, A., Ruano, A., Garcia-Sol, L., van Nunen, E. and van de Wouw, N. (2018) Cooperative Automated Maneuvering at the 2016 Grand Cooperative Driving Challenge. *IEEE Transactions on Intelligent Transportation Systems*, 19, 1213–1226.
- PTV Group (2018). *PTV Vissim 11 User Manual*. Karlsruhe, Germany.
- Rahman, M., Chowdhury, M., Xie, Y. and He, Y. (2013) Review of Microscopic Lane-Changing Models and Future Research Opportunities. *IEEE Transactions on Intelligent Transportation Systems*, 14, 1942–1956.
- Rau, A., Jain, M., Xie, M., Nguyen, T., Liu, T., Liu, X., Zhou, Y. and Ul Abedin, Z. (2019) Planning and Design of a New Dynamic Autonomous Public Transport System: The DART System in Singapore.
- Reina, D.G., Ruiz, P., Ciobanu, R., Toral, S.L., Dorransoro, B. and Dobre, C. (2016) A Survey on the Application of Evolutionary Algorithms for Mobile Multihop Ad Hoc Network Optimization Problems. *International Journal of Distributed Sensor Networks*, 12, 2082496.
- Salvucci, D. (2002). *Modeling Driver Distraction from Cognitive Tasks*.

- Schakel, W.J., Knoop, V.L. and van Arem, B. (2012) Integrated Lane Change Model with Relaxation and Synchronization. *Transportation Research Record: Journal of the Transportation Research Board*, 2316, 47–57.
- Schot, S.H. (1978) Jerk: The Time Rate of Change of Acceleration. *American Journal of Physics*, 46, 1090–1094.
- Sparmann, U. (1978). *Spurwechselforgänge auf zweispurigen BAB-Richtungsfahrbahnen*, Karlsruhe, University. Karlsruhe, Germany.
- Stebbins, S., Hickman, M., Kim, J. and Vu, H.L. (2017) Characterising Green Light Optimal Speed Advisory trajectories for platoon-based optimisation. *Transportation Research Part C: Emerging Technologies*, 82, 43–62.
- Strom, E.G. (2011) On Medium Access and Physical Layer Standards for Cooperative Intelligent Transport Systems in Europe. *Proceedings of the IEEE*, 99, 1183–1188.
- Svensson, L. and Eriksson, J. (2015). *Tuning for Ride Quality in Autonomous Vehicle Application to Linear Quadratic Path Planning Algorithm*.
- Talebpour, A. and Mahmassani, H.S. (2016) Influence of connected and autonomous vehicles on traffic flow stability and throughput. *Transportation Research Part C: Emerging Technologies*, 71, 143–163.
- Toledo, T., Koutsopoulos, H.N. and Ben-Akiva, M.E. (2003) Modeling Integrated Lane-Changing Behavior. *Transportation Research Record: Journal of the Transportation Research Board*, 1857, 30–38.
- Transit Link Pte Ltd. (2016) Electronic Guide - Bus Enquiry. [https://www.transitlink.com.sg/eservice/eguide/service\\_idx.php](https://www.transitlink.com.sg/eservice/eguide/service_idx.php).
- Treiber, M., Hennecke, A. and Helbing, D. (2000) Congested traffic states in empirical observations and microscopic simulations. *Physical review. E, Statistical physics, plasmas, fluids, and related interdisciplinary topics*, 62, 1805–1824.
- TUM CREATE (2020) Towards the Ultimate Public Transport System. <https://www.tum-create.edu.sg/content/towards-ultimate-public-transport-system-0>. Accessed 22.05.2020.
- van Arem, B., van Driel, C.J. and Visser, R. (2006) The Impact of Cooperative Adaptive Cruise Control on Traffic-Flow Characteristics. *IEEE Transactions on Intelligent Transportation Systems*, 7, 429–436.
- Viegas, J. and Lu, B. (2000) The Intermittent Bus Lane Signals Setting within an Area. *IFAC Proceedings Volumes*, 33, 573–578.
- Wiedemann, R. (1974). *Simulation des Strassenverkehrsflusses*. Karlsruhe, Institut für Verkehrswesen der Universität Karlsruhe.

- Xiao, L., Wang, M., Schakel, W. and van Arem, B. (2018) Unravelling effects of cooperative adaptive cruise control deactivation on traffic flow characteristics at merging bottlenecks. *Transportation Research Part C: Emerging Technologies*, 96, 380–397.
- Xie, M., Rau, A. and Fritz, B. (2019) Virtual Right-of-way - Improving the Transit Operation Under Mixed Road Conditions Using Vehicle to Everything (V2X) Techniques, *Proceedings of the UITP Global Public Transport Summit 2019*.
- Zhang, K. and Batterman, S. (2013) Air pollution and health risks due to vehicle traffic. *Science of The Total Environment*, 450-451, 307–316.
- Zhao, W., Ngoduy, D., Shepherd, S., Liu, R. and Papageorgiou, M. (2018) A platoon based cooperative eco-driving model for mixed automated and human-driven vehicles at a signalised intersection. *Transportation Research Part C: Emerging Technologies*, 95, 802–821.

## List of Abbreviations

AV	Autonomous Vehicle
CACC	Cooperative Automatic Cruise Control
CAV	Connected Autonomous Vehicle
DART	Dynamic and Autonomous Road Transit
EBL	Exclusive Bus Lane
HGV	Heavy Goods Vehicle
IDM	Intelligent Driver Model
ITS	Intelligent Transportation Systems
MOBIL	Minimizing Overall Braking Induced by Lane Change
RSU	Roadside Unit
NLC	Number of Lane Changes
VROW	Virtual Right of Way
VANETs	Vehicular Ad Hoc Networks
V2I	Vehicle-to-Infrastructure
V2V	Vehicle-to-Vehicle
V2X	Vehicle-to-Everything

## List of Symbols

$a_{coop}$	$\left[\frac{m}{s^2}\right]$	Cooperative acceleration
$a_{current}$	$\left[\frac{m}{s^2}\right]$	Current acceleration of vehicle
$a_{max}$	$\left[\frac{m}{s^2}\right]$	Maximum allowed acceleration of vehicle
$j_{coop}$	$\left[\frac{m}{s^3}\right]$	Jerk limit for cooperative driving
$t_{TimeStep}$	[s]	Simulation time step
$d$	[m]	(Wiedemann 74) desired safety distance
$ax$	[m]	(Wiedemann 74) standstill distance factor
$bx$	[m]	(Wiedemann 74) velocity-dependent distance factor
$bx_{add}$	[m]	(Wiedemann 74) additive safety distance factor
$bx_{mult}$	[m]	(Wiedemann 74) multiplicative safety distance factor
$z$	-	(Wiedemann 74) stochastic safety distance factor
$\alpha$	-	(IDM) denotes term for ego vehicle
$a$	$\left[\frac{m}{s^2}\right]$	Acceleration
$v$	$\left[\frac{m}{s}\right]$	Velocity
$a^{(\alpha)}$	$\left[\frac{m}{s^2}\right]$	(IDM) maximum allowed acceleration
$b^{(\alpha)}$	$\left[\frac{m}{s^2}\right]$	(IDM) desired deceleration
$\delta$	-	(IDM) acceleration exponent
$s_{\alpha}$	[m]	(IDM) gap to preceding vehicle
$s^*$	[m]	(IDM) desired minimum gap
$s_0$	[m]	(IDM) additive term of minimum desired distance
$s_1$	[m]	(IDM) multiplicative term of minimum desired distance

$T$	$[s]$	(IDM) safe time headway
$v_0$	$\left[\frac{m}{s}\right]$	(IDM) desired velocity
$\Delta v$	$\left[\frac{m}{s}\right]$	(IDM) relative velocity with preceding vehicle
$\dot{v}_\alpha$	$\left[\frac{m}{s^2}\right]$	(IDM) acceleration
$\Delta a_{th}$	$\left[\frac{m}{s^2}\right]$	(MOBIL) acceleration threshold for lane change to occur
$a_n$	$\left[\frac{m}{s^2}\right]$	(MOBIL) acceleration of new following vehicle
$a_o$	$\left[\frac{m}{s^2}\right]$	(MOBIL) acceleration of former following vehicle
$p$	-	(MOBIL) politeness factor
$G_H$	-	GEH calibration statistic
$q$	$\left[\frac{veh}{h}\right]$	Observed traffic flow
$\hat{q}$	$\left[\frac{veh}{h}\right]$	Modeled traffic flow
$GVF$	-	Goodness of Variance Fit
$SDAM$	$[s]$	Sum of Squared Deviations of the Array Mean
$SDCM_{all}$	$[s]$	Sum of Squared Deviations of the Class Means

## List of Figures

Figure 1.1. Concept of the DART system (TUM CREATE, 2020). .....	3
Figure 2.1. Multi-hop transmission of data for a VANET in an urban setting (da Costa et al., 2019). .....	6
Figure 2.2. V2I communication architecture schematic (Bi et al., 2014). .....	6
Figure 2.3. V2X communication architecture for improved signal reliability and traffic management. (Jia and Ngoduy, 2016a). .....	7
Figure 2.4. Merging control of two streams of cooperative vehicles, where $s_e$ is the start point for merging, $d_e$ is the length available for merging, and $v_e$ is the required exit velocity (Mosebach et al., 2016). .....	9
Figure 2.5. Centralized control algorithm for merging streams on a highway. The green arrow indicates the current leader, and the black arrow indicates the planned leader after merging (Ntousakis et al., 2016). .....	9
Figure 2.6. Platoon-based cooperative eco-driving with AVs as lead vehicles (Zhao et al., 2018). .....	11
Figure 2.7. The Wiedemann 74 model's five regimes for car-following behavior (PTV Group, 2018). The behavior corresponding to each regime is mentioned in the text. ....	16
Figure 2.8. Schematic of cooperative driving in Vissim (PTV Group, 2018). .....	18
Figure 3.1. Conceptual operation of VROW with cooperative driving. ....	21
Figure 3.2. VROW and Cooperative Driving Communication Architecture .....	23
Figure 3.3. Modified VROW algorithm, based on Xie et al. (2019), to incorporate cooperative driving behavior. ....	25
Figure 3.4. Impact of including a safety distance reduction factor for lane-changing. ....	27
Figure 3.5. Vehicle following distance as a function of velocity in Vissim .....	29
Figure 3.6. Following distance impact on the ability to create a gap .....	29
Figure 3.7. Cooperative acceleration algorithm. ....	30
Figure 4.1. The study area of Pioneer Road North. The intersection codes were chosen by the LTA and will be used for conciseness to reference specific intersections. ....	34
Figure 4.2. Intersection 8605 of study area showing unsignalized left turn slip roads. ....	35
Figure 4.3. Vissim network model of Pioneer Road North study area. ....	37
Figure 5.1. Acceptable gap related to velocity in the 100% Scenario. Different safety distance functions were used based on certain conditions. The vehicles' cooperative behaviors are also shown. ....	41
Figure 5.2. Gap creation through acceleration and vehicle control of an individual vehicle. ....	43
Figure 5.3. Comparison of jerk values of all vehicles in one simulation run in (a) the 0% penetration scenario and (b) the 100% penetration scenario. ....	45
Figure 5.4. Comparison of acceleration values of all vehicles in one simulation run in (a) the 0% penetration scenario and (b) the 100% penetration scenario. ....	46
Figure 5.5. Northbound travel time distributions and median group travel times for (a) buses and (b) private vehicles at different penetration rate scenarios. ....	48
Figure 5.6. Southbound travel time distributions and median group travel times for (a) buses and (b) private vehicles at different penetration rate scenarios. ....	49
Figure 5.7. Average number of lane changes per vehicle class compared to buses for northbound ( <i>a</i> and <i>b</i> ) and southbound vehicles ( <i>c</i> and <i>d</i> ) for non-connected and connected vehicles. Please note that the points within close proximity to one another have been given a slight offset to improve clarity... ..	53
Figure 5.8. Following distance distribution for 0% and 100% scenarios. ....	55

Figure 5.9. Comparison of bus (a) and private vehicle (b) performance for northbound traffic for the 0% scenario, 100% scenario without cooperative driving, and 100% scenario with cooperative driving. .....	56
Figure 5.10. Comparison of bus (a) and private vehicle (b) performance for southbound traffic for the 0% scenario, 100% scenario without cooperative driving, and 100% scenario with cooperative driving. .....	57

## List of Tables

Table 3.1. Summary of cooperative driving algorithm functions. ....	22
Table 4.1. Summary of calibration results for GEH statistic at each intersection approach per intersection .....	39
Table 5.1. Changes in passenger flow rates at different compliance rates. ....	51
Table 5.2. Changes in passenger flow rates with and without cooperative driving at a 100% compliance rate .	58

## Declaration Concerning the Master's Thesis

I hereby confirm that the presented thesis work has been done independently and using only the sources and resources as are listed. This thesis has not previously been submitted elsewhere for purposes of assessment.

Singapore, June 4th, 2020

---

Michael Winsor